Bioprocess Biosyst Eng (2006) 28: 351–378
DOI 10.1007/s00449-005-0041-0

ORIGINAL PAPER

B. Junker · M. Lester · T. Brix · D. Wong
J. Nuechterlein

A next generation, pilot-scale continuous sterilization system for fermentation media

Received: 6 December 2005 / Accepted: 12 December 2005 / Published online: 18 February 2006

Abstract A new continuous sterilization system was designed, constructed, started up, and qualified for media sterilization for secondary metabolite cultivations, bioconversions, and enzyme production. An existing Honeywell Total Distributed Control 3000-based control system was extended using redundant High performance Process Manager controllers for 98 I/O (input/output) points. This new equipment was retrofitted into an industrial research fermentation pilot plant, designed and constructed in the early 1980s. Design strategies of this new continuous sterilizer system and the expanded control system are described and compared with the literature (including dairy and biowaste inactivation applications) and the weaknesses of the prior installation for expected effectiveness. In addition, the reasoning behind selection of some of these improved features has been incorporated. Examples of enhancements adopted include sanitary heat exchanger (HEX) design, incorporation of a "flash" cooling HEX, on-line calculation of F_o and R_o, and use of field I/O modules located near the vessel to permit low-cost addition of new instrumentation. Sterilizer performance also was characterized over the expected range of operating conditions. Differences between design and observed temperature, pressure, and other profiles were quantified and investigated.

Keywords Continuous sterilizer · High temperature short time · Spiral heat exchanger · Pilot scale · Start-up

B. Junker (✉) · M. Lester · T. Brix
Bioprocess Research and Development, Merck Research Laboratories, RY810-127, P. O. Box 2000, Rahway, NJ 07065, USA
E-mail: beth_junker@merck.com
Tel.: +1-732-5947010
Fax: +1-732-5947698

D. Wong · J. Nuechterlein
Central Engineering, Merck and Company, P. O. Box 2000, Rahway, NJ 07065, USA

Abbreviations

AI	Analog input
AO	Analog output
BI(s)	Biological indicators
CIP	Clean-in-place
DIW	Deionized water
DI	Digital input
DO	Digital output
ESL	Extended shelf life
FV	Filter value
HEX(s)	Heat exchanger(s)
HMI	Human/machine interface
HPM	High performance Process Manager (Honeywell Inc.)
HR	Heat recovery
HTST	High temperature, short time
I/O	Input/output
I/P	Current, I (4–20 mA), to air pressure, P (3–15 psig), transducer
LMTD	Log mean temperature difference
NTU	Number of transfer units
PE	Integrated pasteurization effect
PID	Proportional/integral/derivative
P&ID	Piping and instrument diagram
PSV	Pressure safety valves
PV	Process variable value
RD	Rupture disc
SIP	Steam (sterilize)-in-place
TC	Thermocouple
TDC	(Honeywell) Total Distributed Control
TDH	Total dynamic head
TE	Thermal effectiveness factor
TOC	Total organic carbon
TTI(s)	Time temperature integrator(s)
UHT	Ultra high temperature

List of symbols

A	frequency factor, which varies with molecularity of reaction, min^{-1}
A_{HEX}	heat transfer area of heat exchanger, m^2

C_o	initial tracer concentration, g/L
C_p	specific heat capacity of fluid at constant pressure, kJ/kg-K
C_v	valve constant (sizing coefficient) used to quantify its flow capacity; flow rate of water at 60°F (gal/min) when downstream pressure is 1 psi below upstream pressure
$C(t)$	tracer concentration versus time after pulse input, g/L
D	diameter of retention loop pipe, cm
D_P	diameter of particle, cm
D_T	D-value for hold temperature T, time for one log reduction in spore concentration, min
D_z	axial dispersion coefficient, m^2/s
E_a	activation energy in the Arrhenius equation, kcal/g mol
$E(t)$	tracer concentration versus time for pulse input normalized by area under concentration versus time curve; fraction of fluid elements exiting system having a hold time, t
$F(t)$	tracer concentration versus time for step change normalized by initial tracer concentration; probability that fluid element left system within time t, volume fraction of outlet stream remaining in system for a time less than t
F_o	time at specified sterilization hold temperature T, equivalent to exposure to a saturated steam environment of 121°C for spore inactivation, min
F	Fanning friction factor
h	heat transfer coefficient between particle and fluid, cal/s-cm^2−°C
$k(t)$	thermal death constant as a function of incremental sterilization hold time, t, min^{-1}
K	thermal conductivity, cal-cm/s-cm^2−°C
K_P	gain constant in PID control equation
L	length of pipe, m
N_o	initial concentration of live organisms prior to heat treatment, #/ml
$N(t)$	concentration of live organisms at incremental sterilization time t surviving heat treatment, #/ml
N_{Bs}	Bodenstein number, VL/D_z
N_{Nu}	Nussult number, hD_P/K
N_{Re}	Reynolds number, $DV\rho/\eta$
P	system back-pressure, kg_f/cm^2
Q	system volumetric flowrate, lpm
$Q_{\Delta T}$	Q-value, death rate increase for specified change in temperature, ΔT
Q_M	system mass flow rate, kg/s
R	universal gas constant, 1.987 cal/mol-K
R_o	time at specified sterilization hold temperature, T, equivalent to exposure to a saturated steam environment of 121°C for nutrient inactivation, min
t	incremental sterilization hold time, min
t_i	initial sterilization hold time used for integration boundary, min
t_m	mean sterilization hold time calculated from residence time distribution data, min
t_{max}	maximum sterilization hold time calculated from residence time distribution data, min
t_{min}	minimum sterilization hold time calculated from residence time distribution data, min
t_f	final sterilization hold time used for integration boundary, min
t_o	reference sterilization hold time, min
t_R	total sterilization hold or residence time, min
T_1	integral constant for PID control equation, min per repeat
T_2	derivative constant for PID control equation, min
T	sterilization hold temperature, K or °C
$T(t)$	sterilization hold temperature as function of sterilization hold time t, K
$T_{in,hot,ctr}$	temperature of hot incoming fluid entering in the HEX center, °C
$T_{in,cold,ext}$	temperature of cold incoming fluid entering on the HEX exterior (periphery), °C
$T_{out,cold,ctr}$	temperature of cold outgoing fluid exiting from the HEX center, °C
$T_{out,hot,ext}$	temperature of hot outgoing fluid exiting on the HEX exterior (periphery), °C
T_o	reference sterilization hold temperature, K
Δt	time intervals for residence time distribution profiles, min
ΔT	change in sterilization hold temperature, K or °C
ΔT_{ln}	log mean temperature difference, °C
U	overall mean heat transfer coefficient between the fluid streams, W/s−m^2-K
V	velocity in pipe, m/s or cm/s
V_s	system retention loop volume, L
Z	Z-value, temperature difference which causes a tenfold (one log) change in D_T, K or °C
η	viscosity of fluid being sterilized, cP (0.01 g/cm-s)
σ^2	variance of $E(t)$ distribution
ε	surface roughness, m
ρ	density of fluid being sterilized, kg/m^3
ρ_p	particle density, kg/m^3

Introduction

Continuous sterilization also is known as high-temperature, short-time (HTST) sterilization. A continuous sterilizer heats non-sterile (raw) medium to the desired sterilization hold temperature (typically 135–150°C), maintains it at constant temperature in an adiabatic holding loop (consisting of a long length of insulated

stacked piping connected with *U*-bends for compactness), then cools it to 35–60°C before transferring flow to a fermenter that has been previously sterilized empty or with a minimal amount of water. The residence time that medium is held at sterilization temperature, t_R (min) [calculated from the adiabatic retention loop volume, V_s (L), divided by the system volumetric flowrate, Q (lpm)], is varied by adjusting flowrate and/or length of the holding loop.

Energy is recovered by pre-heating incoming cold medium from 15°C (worst case) to 120°C with outgoing sterilized medium that is cooled from its sterilization temperature of 150 to 45°C prior to entering the process cooler where it is cooled further to 35°C. Medium is recycled back to a circulation tank (also called a surge or recycle tank) or diverted to the sewer during start up or process upsets (such as a decrease in sterilization temperature or an increase in system flowrate). This circulation tank can be pressurized or non-pressurized with the non-pressurized design approach requiring a second "flash" cooler before returning flow to the recycle tank to avoid flashing. Heating is accomplished indirectly using steam or hot water via a heat exchanger (HEX) or directly by mixing steam with incoming medium (steam injection). Cooling HEXs can use cooling tower/chilled water, but also may use vacuum to reduce temperature and draw off any accumulated water from direct steam injection. Continuous sterilization systems typically are pre-sterilized with steam by direct injection and/or with hot water. After attaining steady state with water flow, non-sterile medium feed is introduced. Various media components are sterilized in aliquots and sent to the receiving fermentation vessel with water flushed between them.

A next generation, pilot-scale continuous sterilization system was designed, installed, started up, and validated. Demolition as well as retrofit was accomplished within an actively operating industrial pilot plant. Despite prior experience with a stick-built, internally designed system, a skid-mounted vendor design was selected consisting of five skids (recovery and heating exchangers, hot water loop and exchanger, retention loop, process and "flash" cooling HEXs, and switching valve station). Sterilized medium, obtained from the system at 40–100 lpm, typically was aliquoted into 800–19,000 L scale fermenters with lower flowrates being most appropriate for lower fermenter volumes. The design accommodated a range of different media types, including low solids levels below 5 wt.% and concentrated nutrient solutions.

The design evaluated features from related industrial applications of continuous sterilization, including sanitary design advances in spiral HEX fabrication that were considered helpful. Valued design characteristics were flexibility, reliability, and straightforwardness in operation and maintenance. Although some general papers describing continuous sterilizer design are available [10, 35], there have been few, if any, publications linking design and operation, despite the considerable and varied industrial applications of high temperature, short time (HTST) sterilization. This paper describes the design and testing of a next generation HTST continuous media sterilization system, along with the technical rationale behind its features and flexibility.

Background

Advantages

Advantages of continuous sterilization have been outlined in several reports [3, 7, 10, 30, 60, 84]. By far the most noted benefit is energy conservation since continuous sterilization consumes up to 60–80% less steam and cooling water for large-scale fermenter media volumes. This economy lies at the high end of this range when continuous sterilization utilizes heat recovery via indirect heat exchange to pre-heat incoming cold medium with hot medium leaving the sterilization hold loop. It thus requires less energy (as well as generates a more uniform demand without peak draws [7]); than the alternative batch sterilization process involving sterilizing the fermenter vessel and its non-sterile contents together. Batch sterilization becomes less efficient with scale since heating and cooling portions of the cycle are longer than the constant hold temperature portion [54, 83], and heat transfer coefficients decrease with scale up [34]. Prior to receiving continuously sterilized medium, the fermenter is sterilized empty or with a small volume of water covering the pH and dissolved oxygen probes. Heat up/cool down times are substantially shorter, decreasing overall turn-around time [96].

Continuous sterilization results in gentler treatment of medium compared to batch sterilization, which tends to overheat medium to ensure that vapor space vessel internals achieve sterilization temperatures [1]. Sterilization at higher temperatures for a shorter time generates less degradation of heat-sensitive medium components since spore destruction rates increase faster than nutrient destruction rates as temperature rises [15]. The activation energy for nutrient degradation ranges from 50 to 150 kJ/mol, which typically is smaller than activation energies for the thermal death of microorganisms, which range from 250 to 350 kJ/mol [67]. Consequently F_o increases more than R_o as temperature rises [1, 52]. Similarly, amino carbonyl or Maillard browning reactions, which form objectionable color and tastes to consumers for pasteurization and adversely affect medium quality (destroy growth factors) for fermentation, are minimized [12, 54]. In the case of polymerized poly (L-lactide) rod implants, lower molecular weight decreases also have been found for autoclave cycles at higher temperatures and shorter times [88].

Continuous sterilization results in more uniform heat treatment of medium than batch processes since the system operates at steady state [15]. Proteins and carbohydrates can be separately sterilized in multiple sections using several mix tanks with a sterile water flush between them [96]. Since there is no need to agitate unaerated (ungassed) large liquid volumes during batch

sterilization, fermenter agitator design can be based on drawing full load during gassed conditions [96]. Some feel that continuous sterilization offers a lower contamination rate relative to batch sterilization since fermenter internals are more easily sterilized in an empty rather than full fermenter [96]; others believe that batch sterilization has a lower risk since there is no need to transfer aseptic media [97]. HTST systems have a high degree of flexibility since a large range of time/temperature combinations can be selected within equipment design limits. Scale up is linear with media flowrates of 10–100,000 L/h reported for HTST systems [36] and up to 30,000–50,000 L/h for pasteurizers [38]. Time/temperature exposure profiles accurately reflect sterilization conditions for the media of interest and can be readily modeled. Finally, the ability to design heat exchange equipment to minimize fouling reduces cleanability and maintenance concerns.

Disadvantages of continuous sterilization primarily are that process control performance is critical since it is necessary to immediately divert flow of any inadequately sterilized medium, halt any further medium sterilization, and resterilize the system. In contrast, for a batch sterilization system upset, often additional hold time can be readily added to the sterilization. Continuous sterilizer systems also use dedicated equipment that usually is not well suited for other purposes.

Applications

Several relevant background papers on applications of continuous heat treatment of liquids have been published in the food, biowaste, and fermentation fields.

Applications of continuous sterilization to dairy and other food pasteurization are prevalent in the literature. A continuous pasteurization process with a hold temperature of 72°C and hold time of 15 s replaces a batch process with a lower hold temperature of 63°C for 30 min [65]. Ultra high temperature (UHT) treatment (120–136°C), using either direct steam injection or indirect heating, is used to obtain longer preservation (specifically greater log reduction) than pasteurization at 72°C [32]. Temperatures of 100–145°C produce extended shelf life milk with a product shelf life of 15–30 days at 7°C [16]. Direct steam injection for heating feed to its hold temperature for UHT treatment causes less destruction to other milk components owing to rapid heating using injected steam and rapid cooling using a vacuum [43].

For dairy applications, often the lethality achieved during heat up and cool down periods is similar in magnitude to that achieved during isothermal hold time [67], and thus needs to be considered in evaluating exposure. The integrated pasteurization effect (PE) is calculated to convert the time, t (min), at different temperatures, $T(t)$ (K), in various sections of the pasteurizer (specifically the heat up, holding, and cooling sections), to the equivalent time at a reference temperature, T_o, of 72 C (345 K) and a reference time, t_o, of 15 s (0.25 min) (Eq. 1):

$$\mathrm{PE} = 1/t_o \int_{t_i}^{t_f} [\exp(t - E_a/R)(1/T(t) - 1/T_o)\mathrm{d}t], \qquad (1)$$

where E_a is the activation energy, cal/mol, and R is the universal gas constant of 1.987 cal/mol-K. A PE of one corresponds to complete pasteurization at 72°C for 15 s [65].

The effectiveness of heat treatment in the food industry is established indirectly since it is undesirable to introduce indicator organisms into production equipment. An indicator enzyme such as alkaline phosphatase is used to test proper milk pasteurization after first establishing its relation to pathogen load [28, 65] and pasteurization effect [69]. The behavior of indicator organisms also is examined and rigorously modeled since obtaining accurate kill kinetics at operational conditions can be problematic [72, 80, 87].

Continuous sterilization also is used for biowaste destruction and decontamination of spent broth, the major byproduct from biotechnology plants [41, 84]. Typical sterilization temperatures vary from as low as 80°C up to 140°C, for usually short hold times of 1–5 min. Less aggressive conditions are warranted since organisms being sterilized are active cultures and not dormant spores. Batch systems involve heat up, sterilization, and cool down of waste, all in the same jacketed vessel, and often with direct steam sparging for heating and an external HEX used for cooling to shorten the time cycle [57]. Owing to its higher throughput, continuous sterilization has been applied to biowaste treatment [60], and the prediction that it eventually would be the preferred method of biowaste inactivation [84] has been realized for larger facilities.

Operational concerns for biowaste treatment are opposite those for media sterilization. Although both processes require achievement of the desired log reduction of live organisms in the feed, biowaste treatment is concerned with live organism leakage into either previously sterilized effluent broth and/or uncontained cooling water. In contrast, media sterilization/pasteurization is concerned with live organisms leaking into sterilized media from non-sterile cooling water [98] and/or non-sterile incoming feed.

For fermenter media sterilization applications, continuous sterilization complements continuous fermentation, which can be more productive for certain fermentation processes since it substantially reduces fermenter turn-around time between successive runs [102]. Systems are able to be maintained on-line and ready so that they can continuously sterilize and deliver mid-cycle medium additions directly into active fermentations. Typical sterilization temperatures range from 135 to 150°C with hold times of 4–12 min. Similarly to the PE value for pasteurization, the F_o value (min) is used to characterize sterilization effectiveness for fermentation medium [18]. It is the time for the

actual sterilization hold temperature that is equivalent to exposure to a saturated steam environment of 121°C, according to Eq. 2:

$$F_o = \int_{t_i}^{t_f} [10^{(T(t)-121.1)/Z} dt], \quad (2)$$

where $T(t)$ is the sterilization hold temperature, K, t is the incremental sterilization hold time, min, integrated over the start time, t_i, to finish time, t_f, and Z is the temperature difference (K or °C) for a one log change in D_T (min), the time for a one log reduction in spore concentration. A similar expression can be developed for the analogous impact on nutrient degradation, R_o (min) [17].

High temperature, short time continuous heat treatment also has been evaluated for the viral inactivation of mammalian cell culture medium (hold temperature of 102°C and hold time of 10 s) to minimize nutrient degradation [66] and of blood plasma (hold temperature of 77°C and hold time of 0.006 s) to maintain protein structure and activity [23].

Kill/degradation kinetics

Relative to *Escherichia coli*, the heat resistance of bacterial spores is 3 million:1, mold spores is 2–10:1, and viruses and bacteriophages is 1–5:1 [34]. As a first pass, the kinetics of kill and degradation are based on the Arrhenius equation for the thermal death constant, $k(t)$, min^{-1} (Eq. 3) as a function of the incremental sterilization holding time, t:

$$k(t) = A_{exp}[-E_a/(RT(t))] \quad (3)$$

where $T(t)$, E_a, and R are defined as in Eq. 1 and A is the frequency factor of the reaction, min^{-1}. Adherence to strict first order kinetics is not always the case [4, 33], and this model does not incorporate partial germination and/or heat activation of dormant spores prior to media sterilization reducing their heat resistance [90]. Nevertheless, this simple model is employed for the validation of media sterilization conditions in the fermentation industry.

Using the Arrhenius model, the non-temperature dependent activation energy can be calculated from the regressed slope of log of reaction rate constant versus the reciprocal of absolute temperature [67]. Typical values for *Bacillus (Geobacilllus) stearothermophilus*, an indicator organism commonly used to evaluate heat treatment effectiveness, are 9.5×10^{37} min^{-1} for A and 70,000 cal/mol for E_a [11].

The D value, D_T (min), or decimal reduction time, is the time to decrease the population to one-tenth its original number at a specified temperature [15]. The Z value (K or °C) is number of degrees of temperature rise that causes a tenfold increase in D value [15]. It is obtained by plotting the log of the D value versus the corresponding temperature and calculating the Z value obtained from the reciprocal of the slope of the least squares regression line (Bigelow model) [67]. The $Q_{\Delta T}$ value is the death rate increase for a specified change in temperature, ΔT [15], and it is calculated from the dependence of the D value (specifically k) on temperature. Both D and Z values are affected by the physicochemical and biochemical properties of the solution to be sterilized (e.g., composition, pH) [21, 51, 52, 85, 101].

The Z value for *B. stearothermophilus* in water is 10°C, vs. 56°C for vitamin B_1 and 50°C for vitamin B_2 (riboflavin) [15], both notably higher. Correspondingly, the Q_{10} value for *B. stearothermophilus* is 11.5, vs. 2.1 for vitamin B_1, 2.3 for vitamin B_2 (riboflavin), and 3.0 for the Maillard reaction [15], all notably lower. Two models (Arrhenius or Bigelow) can be used to extrapolate death rates for higher temperatures than those measured experimentally since it is difficult to measure kill and degradation kinetics at temperatures above 130°C with existing equipment [67].

Using the overall sterilization hold time or residence time, t_R, the log reduction may be obtained according to Eq. 4:

$$\log (N(t)/N_o) = t_R/D_T, \quad (4)$$

where $N(t)$ is the number of spores surviving heat treatment at incremental sterilization time, t, N_o is the initial number of spores, and D_T is defined below Eq. 2. Assuming $D_{121} = 3$ min and $Z = 10$°C (typical values for *B. stearothermophilus* spores in water [52]), then log reductions for continuous sterilization at 150°C range from 1,800 to 7,500-fold for the system residence times of 5.4–22.5 min, substantially higher than what is obtainable via batch sterilization. Actual sterilization conditions are selected based on specific medium properties and fermentation process requirements.

Retention loop flow behavior and its impact

Flow through a pipe is characterized by the Reynolds number, N_{Re}, given by $DV\rho/\eta$, which is the ratio of inertial to viscous forces. Since the system flow tube diameter, D (cm), does not change, N_{Re} varies with sterilization fluid velocity, V (controlled by system flowrate), fluid viscosity, η (cp), and density, ρ (g/cm^3), which is fixed for the selected medium. As flow becomes more turbulent (higher N_{Re}), flow behavior approaches ideal plug flow.

There is considerable disparity in the literature regarding the Reynolds numbers associated with laminar and turbulent flow through a tube for various continuous flow sterilization applications. For flow through a tube, laminar flow was below 1,100 and turbulent flow was above 2,100 [95]. Laminar flow was below 2,100, and turbulent flow above 4,000 according to another study [81]. A minimum velocity, which gives turbulent flow is recommended with a Reynolds number of about 3,000 [96] or at least 2,500 [30], but

preferably above 20,000 [30]. For a retention loop in a dairy application, Reynolds numbers of 1,130–2,300 were considered laminar [67], and Reynolds numbers of 4,800–7,080 were considered transitional [74]. Substantially higher Reynolds numbers of 7,200–9,400 were considered transitional for the heating and cooling sections of tubular HEXs for a dairy application [67]. Differences in tube roundness and entrance effects may have an influence [68]. System design for N_{Re} well above 10,000, particularly in the holding tube, minimizes potential for inadvertent operation in the laminar flow regime. One potential design approach is to incorporate flow disturbances to induce turbulence at lower N_{Re}. Confirmation of turbulent flow, based on the deviation between ideal and non-ideal plug flow behavior for specific operating conditions, can be determined experimentally.

Continuous thermal treatment is most uniform when the flow through the retention loop is turbulent since residence times of individual streamlines become less variable. The parabolic velocity profile associated with laminar flow leads to variable residence times [67]. Specifically, for laminar flow the mean velocity of a viscous fluid through a pipe is one-half of the maximum velocity along the axis, and for turbulent flow, the mean velocity is 82% of the maximum value [3]. Thus, there are concerns about laminar flow for viscous solutions in pasteurization (e.g., ice cream mix, egg nog, and liquid egg products) [81].

Non-ideal flow behavior is problematic since each fluid element spends different lengths of time in the sterilizer hold phase and thus receives different levels of sterilization. Consequently, it is necessary to characterize the residence time distribution to accurately predict lethality [95], specifically the spectrum of times spent in the sterilizer hold tube for different fluid elements. The extent of the distribution dictates the degree of axial or Taylor dispersion, i.e., concentration gradients along the length of the retention loop. [Radial gradients are assumed negligible]. The holding efficiency, t_{min}/t_m, is evaluated by comparing the minimum holding time, t_{min} (min), to the mean holding time, t_m (min), and the extent of product overheating, t_{max}/t_m, can be calculated using the ratio of the maximum, t_{max} (min), to mean holding times [55].

Stimulus-response measurement techniques and data analysis to determine the extent of non-ideal flow have been described comprehensively [61, 62, 95]. After a pulse or step change is introduced, tracer concentration is measured as a function of time by sampling effluent at the system outlet. The total area under the concentration versus time curve then is calculated and used to normalize concentration measurements so they can be readily compared for different tracer tests.

The exit age distribution, $E(t)$, delineates the fraction of fluid elements exiting the system having a particular hold time, t. It characterizes instantaneous pulse changes (delta function) in tracer concentration. This curve is normalized by dividing measured $C(t)$ values by the area under the resulting concentration versus time curve to obtain $E(t)$, for which the area under the $E(t)$ curve is always one [61].

For $E(t)$ curves, the mean time, t_m, is the sum of individual products of time, normalized tracer concentrations, and time interval, Δt (min), which is assumed constant [46]. The distribution variance, σ^2, is given by Eq. 5:

$$\sigma^2 = \left[\sum_{t_i}^{t_f} (t^2 \times E(t) \times \Delta t)\right] - t_m^2, \tag{5}$$

where $t_m = \sum_{t_i}^{t_f} (t \times E(t) \times \Delta t)$. The dimensionless variance, σ^2/t_m^2, can be used to estimate the dispersion coefficient based on experimental data.

Another concentration versus time curve, $F(t)$, is the probability that a fluid element left the system within time, t, or the volume fraction of the outlet stream that has remained in the system for a time less than t [95]. It characterizes behavior resulting from step inputs of tracer with an initial entering concentration, C_o. The ratio of $C(t)/C_o$ versus time produces a normalized $F(t)$ curve for which the axes range from 0 to 1 [61].

These distributions are related mathematically according to Eqs. 6 and 7:

$$E(t) = \mathrm{d}F(t)/\mathrm{d}t. \tag{6}$$

$$F(t) = \int_0^t E(t)\mathrm{d}t. \tag{7}$$

Integration of $E(t)$ curve to obtain the corresponding $F(t)$ curve via Eq. 7 is accomplished graphically for various Δt [95].

Both the $E(t)$ and $F(t)$ curves also can be made dimensionless in time by normalizing by the mean hold time, t_m. Normalization with respect to time is helpful to compare conditions at different residence times, and normalization with respect to concentration assists in comparing data from different tracer experiments.

The sterilization efficiency for a given residence time distribution is given by Eq. 8:

$$N(t)/N_o = \int_0^t \exp(-kt)\, E(t)\mathrm{d}t. \tag{8}$$

This equation permits quantitative assessment of the sterilization impact from non-ideal flow patterns.

The Bodenstein number (or Peclet number or Peclet-Bodenstein number [3, 54]), N_{Bs}, is given by VL/D_z, where D_z is the axial dispersion coefficient, m^2/s, V is the flow velocity, m/s, and L is the retention loop length, m. This dimensionless group is the ratio of convective transport to axial dispersion [63, 94], and it is used to quantify the extent of axial dispersion. For $N_{Bs} >> 1$, there is plug flow with minimal axial mixing and sterilization efficiency is the highest possible [62, 63]. For $N_{Bs} << 1$, axial dispersion is at its worst, with retention loop contents completely mixed along the tube length, and sterilization likely is incomplete. Actual operating conditions fall between these two extremes [63]. The flow system should be designed so that dispersion is minimized with high N_{Bs}

and high N_{Re} [54], preferably $N_{Re} > 2\times10^4$. N_{Bs} of 3–600 have been reported as typical for continuous sterilizers [30]. The current system's N_{Bs} of about 1.8×10^4 is much higher than this range, most likely due to its longer retention loop.

Experimental distribution data may be used to calculate σ^2/t_m^2, N_{Bs}, and then D_z [61, 62] using Eqs. 9 and 10. For $D_z/VL << 1$ and a normal (Gaussian) distribution for the $E(t)$ curve:

$$D_z/VL = 0.5\sigma^2/t_m^2. \quad (9)$$

Alternatively, the dispersion coefficient and residence time distribution may be inferred from correlations. For turbulent flow, Eq. 10 applies:

$$D_z/VD = 3.57f^{0.5}, \quad (10)$$

where the Fanning friction factor, f, for the retention loop pipe is obtained from correlations based on the ratio of surface roughness, ε, to pipe diameter, D [78]. An experimental correlation for water, where $D_z/VD = 0.25$ for $N_{Re} = 10^5$ and $D_z/VD = 0.33$ for $N_{Re} = 10^4$ [61], was used to assess the reasonableness of measured D_z/VL values and to compare N_{Bs} values obtained using Eqs. 10 and 11a. Friction factors for the retention loop pressure drop, applicable for both laminar and turbulent flow, were calculated using Eq. 11a [26, 75] and shown in Table 9:

$$f = 8[(8/N_{Re})^{12} + (A+B)^{-1.5}]^{1/12}, \quad (11a)$$

where $A = 2.457\ \ln(1/[(7/N_{Re})^{0.9} + 0.27\varepsilon/D])^{16}$ and $B = (37530/N_{Re})^{16}$.

Alternatively these friction factors can be estimated using the Colebrook equation, Eq. 11b [29, 78] and solving iteratively, but this approach was not used:

$$1/(f)^{1/2} = -2.0\log_{10}[12\varepsilon/(3.7D) + 2.51/(N_{Re}(f)^{1/2})]. \quad (11b)$$

Rule-of-thumb conditions generating a narrow residence distribution and low dispersion coefficient for flow through a pipe are $L/D > 200$ and $N_{Re} > 12{,}000$ [55].

Influence of solid content of media

For sterilizer feed medium that contains solids, ranging from small amounts to in excess of 10 vol.% [31], solids must be adequately wetted and dispersed without clumps. Particles flow at different velocities through the retention loop, and temperature distribution within a particle is challenging to monitor. Although it is somewhat straightforward to determine residence time distributions, partial differential equations using finite differences are required to model convective–conductive heat transfer between the fluid and particles [20]. Thermal properties of the surrounding fluid are less critical for heat transfer to particles since the heat transfer coefficient, h (cal/s-cm^2–°C), between the fluid and particle is limiting [59]. Its effectiveness is shown by the Nusselt number (ratio of total heat transfer to conductive heat transfer), N_{Nu}, given by hD_p/K, where D_p (cm) is the particle diameter, and K (cal-cm/s-cm^2–°C) is the thermal conductivity of fluid at the processing temperature [22, 49]. If the predicted particle temperature profile is hotter than the actual one, it is possible to obtain incomplete inactivation [20].

The sterilization challenge of large diameter solids is to avoid selecting hold times/temperatures that sterilize solids but damage liquid medium components [89]. The time required for particles to attain sterilizing temperature is on the order of microseconds for particles several microns in size (i.e., media bioburden) and seconds for solids several millimeters in size (i.e., raw material particles), highlighting the need to clarify raw materials [3, 30]. Time-temperature integrators have been developed to quantify the heating impact on spores within the entire particle. These indicators are spores immobilized in alginate cubes or polymethylmethacrylate designed to have a mechanical resistance to flow through the system similar to that of actual particles [49, 73]. Other tracers have been found to mimic the flow behavior of microbial cells except when the flow is laminar [2].

As the solid content increased from 0 to 30 w/w.%, the mean residence time of the liquid phase increased by 40% and flow less resembled plug flow which indicated that the presence of solids can significantly influence liquid phase flow patterns [76]. Consequently, a safe design approach for solids-containing medium sterilization uses the maximum rather than average fluid velocity [8, 9]. Residence time distributions for solid particles also often have more than one peak representing different groups of particles.

Experimental methods to quantify axial dispersion

Testing of dispersion has been done using a variety of tracers, most commonly salts and dyes. Experimental mean residence times calculated from salt tracer measurements in skim milk were close to the average holding time [74]. A salt tracer was found to be adequate for low viscosity and Newtonian fluids only; it overestimated thermal exposure in more viscous fluids [81]. Salt tracers can be saturated sodium chloride solutions, but chloride exposure is not desirable for stainless steel [50]; thus, other salts with high aqueous solubilities (sodium sulfate, sodium citrate, and magnesium sulfate) and/or sodium hydroxide can be substituted. Dye tracers include fast green FCF (Sigma; St. Louis, MO, USA) and basic Fuchsin (no vendor given) [46].

Other tracers have been based on chemical reactions, specifically sucrose inversion (hydrolysis to glucose and fructose) when heated in an HCl solution at pH 0–2 or sulfuric acid at a pH of 2.5 to avoid exposure of stainless steel to chlorides. Changes in optical rotation and freezing point were used to quantify reaction extent [1]. Another tracer used has been the pulse injection of

20 w/w% citric acid and subsequent pH measurement [76]. Finally, temperature spikes also have been effective tracers in scraped surface HEXs [44].

Overview of operation

A comparison of major changes between the prior and next generation pilot-scale, continuous sterilization systems, as well as expected benefits/risks or potential drawbacks, are summarized in Table 1. A schematic of major equipment components and their arrangement is shown by Fig. 1. System specifications and design criteria are listed in Table 2. After system design was completed for water, its effectiveness was evaluated for concentrated nutrients, typically sterilized separately from the base medium to avoid Maillard reactions or sterilized just prior to delivery to active fed-batch fermentations to avoid storage in a holding tank. The nutrients and concentrations selected were 55 wt.% cerelose (glucose monohydrate; CPC International, Argo, IL, USA) and 50 vol.% glycerol (Superol glycerine; Proctor and Gamble Chemicals, Cincinnati, OH, USA). Physical properties for these test media at various temperatures were estimated for water from [37, 42, DIPPER database tables (dippr.byu.edu)]. Physical properties for 50 vol.% glycerol and 50 wt.% cerelose were modeled using Aspen Plus (AspenTech, Cambridge, MA, USA) process simulation software with physical properties database information.

The sterilizer had several distinct phases that are depicted by Fig. 2 and described briefly below: System start up included (1) leak tests of the cold system under pressure, (2) flowrate and totalizer accuracy checks versus a decrease in feed tank volume, and (3) leak re-check after raising the system to sterilization temperature. Proper operation and reliability of instrumentation was assured by evaluating all pressure

Table 1 Comparison of major changes in large continuous sterilization system

Item	Prior design	New design	Expected benefit/Risk or potential drawback
Final heating method to attain sterilization temperature	Direct steam injection	Indirect heating loop	Less dilution, improved stability with respect to source steam fluctuations, no adulteration from plant steam additives/higher cost
Flowmeter	Magnetic	Coriolis	Ability to sense deionized water/position of flag critical
Number of different retention loop lengths	Able to increase/decrease by two tubes for 16–30 tubes (t_R = 4.0–12.5 min), removable connections at both ends of all tubes	Five configurations from 18 to 30 tubes (t_R = 5.4–22.5 min), removable jumpers at same end of selected tubes	Fewer fittings/limited visual inspection
Flowrate turn down	60–100 lpm	40–100 lpm	Avoids separate smaller unit/multiple ranges for tuning control
Pressure safety device	Safety valve only	Rupture disc and safety valve with tell-tale pressure gauge	Sanitary disc in process contact, evident when disc blown/added cost and maintenance
Second cooler of same size as process cooler (“flash” cooler)	Absent	Present	Ability to conduct water sterilization, installed marker for process cooler/extra expense
Booster pump with pressure control on recuperator outlet	Absent	Present (used with centrifugal feed pump only)	Sterile media at higher pressure than non-sterile media/increased complexity of tuning and operation
Retention loop insulation	Insulated box without packing, 4–6°C temperature drop	Insulated box with packing, < 2°C temperature drop	More adiabatic and isothermal/modest additional expense
HEX plate thickness	1/4″	3/16″	Lower cost and higher surface area per unit volume/higher risk of breach
HEX aspect ratio			
Recuperator	2.7	3.46	Higher velocities/increased effect of channeling due to gap and drain notches
Coolers	4.76	2.91	
Heater	0.93 (horizontal cross flow for condensing service)	1.31	
HEX process side channel thickness	0.25″ (coolers 0.375″)	0.25″ (coolers 0.25″)	Higher surface area per unit volume/higher pressure drop
HEX utility side channel thickness (coolers)	0.75″	0.5″	Higher surface area per unit volume/higher pressure drop

Aspect ratio is the HEX diameter divided by its width

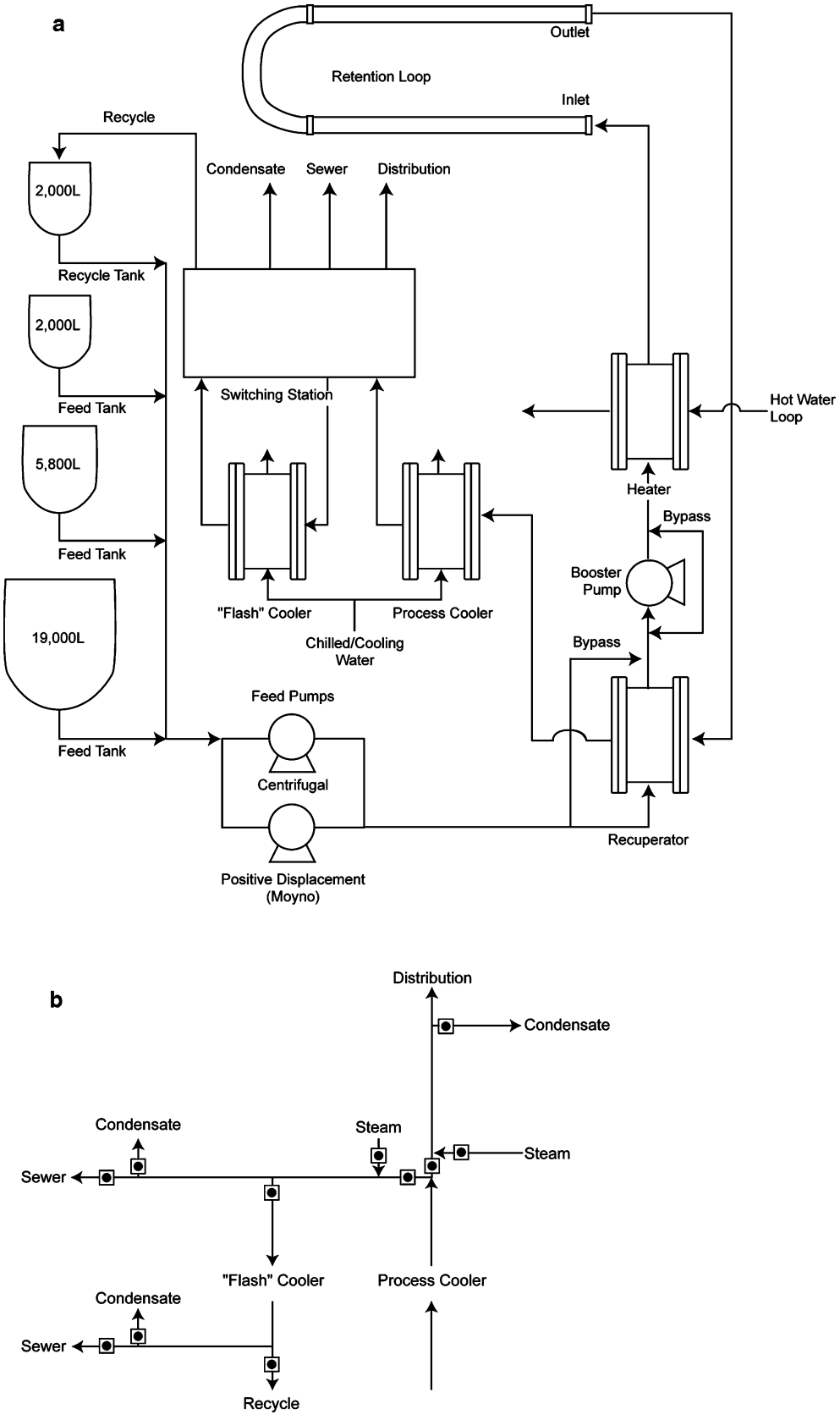

Fig. 1 Schematic of sterilizer system. **a** major components, **b** switching station

and temperature transmitter and gauge readings for consistency. Prior to system sterilization and before introducing steam or superheated water, draining of process water, supplemented by evacuating with 90 psig air, was necessary for preventing stress corrosion cracking of HEXs [93].

The next phase was steam sterilization using four high point steam injection points, one of which was located at the outlet of retention loop, and setting the hot water heating loop to 135°C, slightly above the corresponding steam sterilization temperature of 134°C for the 30 psig (2.1 kg_f/cm^2) steam supplied. After 2 h of steam sterilization, the system was transitioned from steam to water carefully (over a period of 1 h) to maintain sterility, or with less care assuming that water sterilization was planned next. Steam sterilization could be conducted for the system up through the process cooler as well as up through the "flash" cooler (Fig. 1a). Use of the "flash" cooler was the preferred configuration since it provided an extra buffer during steam collapse.

During this next phase of steam-to-water transition, the system flowrate was started with 15 lpm water flowing to the sewer after the "flash" cooler using the Moyno pump. All steam injection points, such as the medium distribution system, were closed, and the hot water generated by the heater provided sufficient back-pressure. The system was set up for water sterilization (i.e., recuperator non-sterile side bypassed and the "flash" cooler used to cool sterilizing water so that the process cooler could be sterilized), and the hot water loop was set at 150°C in cascade (set point for water sterilization). As water entered the system, the temperature of the retention loop rose from 133 to 150°C, while the temperature of the process cooler fell from 148 to 122°C. (The temperature drop of the process cooler was not a sterility risk since the entering 15 lpm water flowrate, sterilized at 133°C, resulted in a sufficient F_o of 965 min to assure sterility of the retention loop effluent). Loss of incoming water due to boiling while the system was at a lower backpressure was believed minimized by the nearly closed "flash" cooler backpressure valve (expected fill volume 1,215 L, actual volume 1,218 L).

During water sterilization, incoming cold water was circulated for two passes (one pass if system was already hot from steam sterilization) at 60 lpm using the centrifugal inlet feed pump, after it rose to the sterilization inlet hold temperature of 150°C. It required previously steamed-through system block/drain valves since users were not comfortable that conduction adequately sterilized through them when closed. The non-sterile side of the recuperator HEX was bypassed to ensure that the sterile side reached sterilization temperature. Cooling water was applied to the "flash" cooler to ensure that the process cooler attained sterilization temperature. For the target sterilization temperature of just below 150°C and a 60 lpm water flowrate, the temperature reached about 148.5°C at the sterile side of the recuperator and 146.5°C for the sterile side of the process cooler.

Water sterilization was redone during medium sterilization if medium diversion was necessary owing to system sterility upset. After taking immediate action to divert media away from the production vessel, water re-sterilization was conducted by (1) diverting flow through the "flash" cooler and enabling its pressure control loop, (2) fully opening the process cooler back-pressure valve, (3) conducting water re-sterilization, (4) enabling the process cooler pressure control loop, (5) fully opening the "flash" cooler back-pressure valve, and then (6) resuming medium sterilization. When switching from the "flash" to the process cooler, it was necessary to maintain sterile conditions.

After the system was sterilized and running on water, typically in recirculation mode or emptying into the system sewer, the switching valve station was used to divert flow to distribution. Water now flowed to a waste vessel or the process sewer located near the eventual medium receiving vessel. After conditions stabilized, sterilizer inlet feed was switched from water to medium. Again, after conditions stabilized, flow was switched to the receiving vessel. When the receiving vessel was filled sufficiently, sterilizer effluent was switched back to the waste tank, sterilizer inlet feed was switched back to water, and then effluent switched back to either the recirculation vessel or system sewer. After media sterilization, a thorough water rinse was conducted at sterilization temperature and the system was cooled to 60°C for cleaning. Alkaline and/or acid cleaning solutions were used depending on the nature of the soil. After cleaning, the system was cooled and drained completely.

Equipment design

The system's five skids were designed and fabricated at the vendor's shop and delivered with only field installation of interconnecting piping required. To minimize design miscommunications, three-dimensional piping models were used for skid piping plans, which were able to be reviewed remotely by the customer. Ball valves were used instead of diaphragm valves for hot temperature service. Hazardous energy control was carefully considered with locking devices installed and valve placement selected for facile equipment isolation and operability. Equipment was citric acid-passivated after installation.

Each relief device on the process side consisted of a flanged rupture disc (RD) with a pressure indicator and telltale as well as a pressure safety valve (PSV) that reseated after the source of excessive pressure was removed. These devices were placed directly after the positive displacement Moyno (Robbins and Myers; West Chester, PA, USA) system inlet feed pump, recuperator outlet, and booster pump. Discharges were piped to return to the feed tank for safety as well as for medium recovery. Piping was designed such that no PSV devices were required on the process side to minimize risk of system integrity disruption. Sample points were located on the inlet feed (pre-sterilization, prior to recuperator) and sterilized medium outlet (post-sterilization, after process cooler) lines.

Heat exchangers

The chief goals of HEX design are to optimize cost, heat transfer, size, and pressure drop [48]. The type of HEX

selected was a spiral, which was preferred over alterative shell and tube, plate and frame, or concentric double pipe designs. A spiral HEX consists of two long, flat, preferably seamless sheets of metal plate, separated by spacers or studs, wrapped around a center core or mandrel which forms two concentric spirals. Alternate ends are welded (both by machine and manually) to create separated flow channels. Hot fluid enters the center (flows inside to outside) and cold fluid enters on the exterior (flows outside to inside) to achieve countercurrent flow. Details of spiral HEX design are described elsewhere [71].

Advantages of spirals are chiefly that they require less space per unit of heat transfer surface area [104]. Their continuously curved channel, unrestricted flow path, and presence of spacers increases turbulence due to secondary flow effects which maintain solids in suspension [13, 103]. Fouling is lower than shell and tube designs since cross-sectional velocities increase as channel size decreases, creating a scrubbing effect [13, 19]. (In contrast, as individual tubes of shell and tube exchangers plug, flow is diverted into unplugged tubes.) Spirals are particularly well suited for slurries and many viscous fluids [103]. Specifically, slurries can be processed at velocities as low as 2 ft/s (0.61 m/s) [71]. Periodic, thorough cleaning can be conducted by simply removing the cover to expose the spiral cavities and cleaning with a high pressure water source.

Evaluation of thermal effectiveness can be done by calculating the number of thermal transfer units, NTU [25, 100], using Eq. 12:

$$\begin{aligned} \mathrm{NTU} &= \mathrm{UA_{HEX}}/Q_{\mathrm{M}}C_p, \\ &= (T_{\mathrm{out,cold,ctr}} - T_{\mathrm{in,cold,ext}})/\Delta T_{\mathrm{ln}}, \\ \Delta T_{\mathrm{ln}} &= [(T_{\mathrm{out,hot,ext}} - T_{\mathrm{in,cold,ext}}) \\ &\quad - (T_{\mathrm{in,hot,ctr}} - T_{\mathrm{out,cold,ctr}})]/ \\ &\quad \ln[(T_{\mathrm{out,hot,ext}} - T_{\mathrm{in,cold,ext}})/(T_{\mathrm{in,hot,ctr}} \\ &\quad - T_{\mathrm{out,cold,ctr}})], \end{aligned} \tag{12}$$

where A_{HEX} is the heat transfer area, m^2, Q_{M} is the mass flow rate (kg/s), U (W/s−m^2-K) is the overall mean heat transfer coefficient between the fluid streams, and C_p (J/kg-K) is the specific heat capacity of the fluid at constant pressure. This quantity also can be obtained from individual stream temperatures where $T_{\mathrm{in,hot,ctr}}$ is the temperature of the incoming hot stream entering in the center, $T_{\mathrm{in,cold,ext}}$ is the temperature of the incoming cold stream entering on the periphery, $T_{\mathrm{out,hot,ext}}$ is the temperature of the outgoing hot stream exiting on the periphery, and $T_{\mathrm{out,cold,ctr}}$ is the temperature of the outgoing cold stream exiting in the center. In this case, the temperature rise of the cold stream is divided by the log mean temperature difference (LMTD) for the HEX. An NTU of 1.0 correspond to a shell and tube HEX; NTU > 1 represents overlap of hot and cold side temperature ranges indicative of spiral HEXs.

Thermal effectiveness also can be evaluated using Eq. 13 to calculate the thermal effectiveness factor, TE [25, 100]:

Table 2 System specifications and design criteria

Parameters	Design range (min–max)
Sterilization hold temperature (T)	135–150°C
Retention loop hold up volume (V_s)	540–900 L
Flowrate (to achieve design recuperator HEX heat recovery) (Q)	40–100 lpm at 15–60°C (water) 40–100 lpm at 60°C (55 wt.% cerelose) 40–65 lpm at 25°C (55 wt.% cerelose) 40–91.5 lpm at 25–60°C (50 vol.% glycerol) 40–88 lpm at 15°C (50 vol.% glycerol) Flow rates < 40 lpm may not achieve sufficient back-pressure for the selected sterilization temperature to avoid flashing
Feed temperature ($T_{\mathrm{in,cold,ext}}$)	15–60°C (water, 50 vol.% glycerol) 25–60°C (55 wt.% cerelose) Feed temperature of 15°C for 55 wt.% cerelose insufficient to maintain a solution
Residence time (t_{R})	5.4–22.5 min
Back-pressure (P)	3.5–5 $\mathrm{kg_f/cm^2}$ (typically 4.1 $\mathrm{kg_f/cm^2}$) Sufficient pressures used to avoid flashing > 2.15 $\mathrm{kg_f/cm^2}$ for 135°C > 3.93 $\mathrm{kg_f/cm^2}$ for 150°C
Retention loop temperature drop (900 L volume and inlet temperature of 150°C), ΔT	2.0°C for 40 lpm, 1.5°C for 60 lpm, 1.0°C for 80 lpm, and 1.0°C for 100 lpm
Heat recovery (HR)	> 70–80% depending inlet feed temperature, media type and flowrate 78.9% (100 lpm water, 60°C) 75.5% (100 lpm 55 wt.% cerelose, 60°C) 78.9% (91.5 lpm 50 vol.% glycerol, 60°C)

$$TE = (T_{out,cold,ctr} - T_{in,cold,ext})/(T_{in,hot,ctr} - T_{out,cold,ctr}). \quad (13)$$

Overall Eq. 13 represents the change in recuperator cold side stream temperature divided by the temperature difference of streams flowing through its center connections (i.e., incoming, sterilized, hot medium exiting retention loop and outgoing, pre-heated, non-sterile medium).

Finally, thermal effectiveness can be evaluated by calculating the heat recovery, heat recovery (HR), using Eq. 14:

$$HR = (T_{out,cold,ctr} - T_{in,cold,ext})/(T - T_{in,cold,ext}) \times 100\% , \quad (14)$$

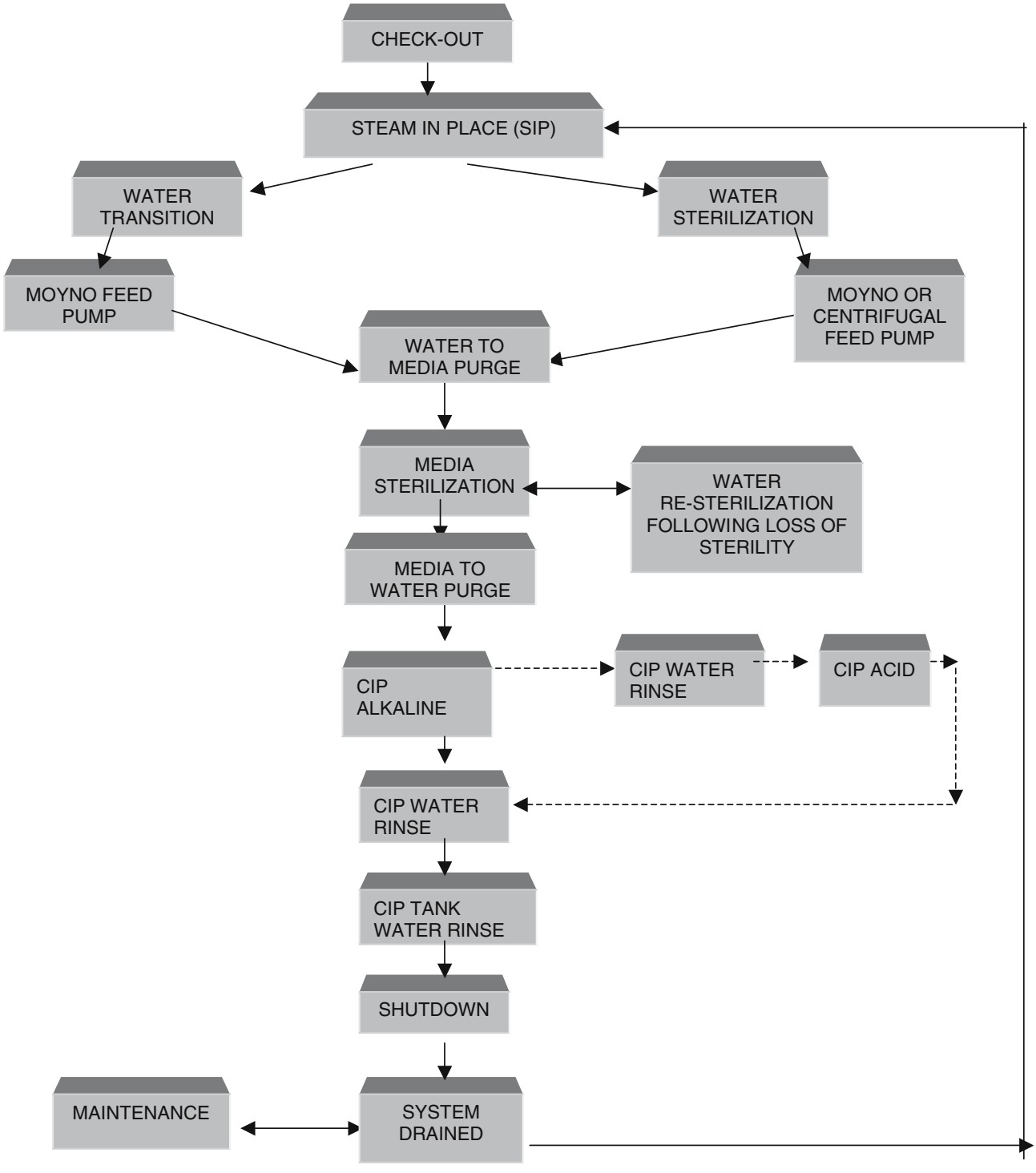

Fig. 2 Overview of sterilizer phases

which represents the heat gained by the incoming cold medium after passing through the recuperator divided by total heat gained by the cold medium after passing through both the recuperator and heater HEXs. Heat recoveries improve with clean HEXs (higher heat transfer coefficient), lower flowrates (permitting more time for heat transfer), and higher inlet feed temperatures (lower medium viscosity which improves heat transfer coefficient). When the temperature difference on both sides of the recuperator is the same, then NTU is replaced by TE, and Eq. 12 cannot be used since $\Delta T_{\ln} = 0$ [14].

For consistency in comparing design and observed performance over the entire sterilizer system, the value of $T_{\text{in,hot,ctr}}$ (retention loop outlet temperature) used for calculating design values in Eqs. 12, 13, and 14 was assumed to be identical to the retention loop inlet temperature (T), i.e., the retention loop was assumed to be isothermal (adiabatic). The sensitivity of these three parameters to small temperature measurement errors of ± 1°C for the expected temperature change of each HEX stream was estimated $\pm 5.7\%$ for NTU, $+3.5/-12.5\%$ for TE, and $\pm 3.0\%$ for HR.

Specific limiting performance case scenarios depend on media type and inlet feed temperature. Higher inlet feed temperature (60°C) is worst case for the cooling HEX since the recuperator removes less heat from sterile medium. Lower inlet feed temperature (15°C) is worst case for the recuperator since it represents the greatest challenge to HR.

Heat exchanger design and material selection is important to extending the unit's lifetime. A pressure rating of 150 psig was selected to match piping specifications, specifically flange connections. Thicker gauge material permitted wider spacing of studs, directly affecting cost [58], minimized corrosion without significantly reducing heat transfer [13], but decreased HEX surface area per unit volume (Table 1). All HEXs underwent hydrostatic as well as helium leak tests. Studs for spacing were only partially welded around the base so a small crack existed. These crevices were considered unavoidable, and they were accepted since they were shallow enough to permit adequate contact with sterilizing and cleaning fluids.

Heat exchanger diameter, width, and channel spacing were designed to minimize fouling and deposits by ensuring channel velocities were sufficiently high during operation. Channel widths of ¼″ were used, except for the utility sides of cooler HEXs, where a channel width of ½″ was selected to minimize plugging due to cooling water deposits and to reduce pressure drop. Bulk velocities for each process fluid are shown in Table 10.

A sanitary design was utilized with a continuous sheet for coil formation, a tapered channel transition for the medium inlet and outlet, external bracing of shell connections, back-welding of the center pocket stiffener as much as possible, elimination of additional center stiffeners, and polishing/cleaning of all internal welds. Process connections were 150 psig bolted, milled, lap-joint flanges possessing a right angle rather than a bevelled edge to line up directly with the gasket and avoid crevices. A solid 316 L stainless steel door eliminated a process side weld around the center nozzle required to attach a stainless steel skin to a carbon steel door.

Heat exchangers initially were designed to include a gap between the spiral face and cover to minimize gouging of the door due to distortion or telescoping. Spirals can "grow" during thermal cycling and cut into full-face gaskets, if present [71] or door covers if annular gaskets were utilized without a sufficient gap. Telescoping also was minimized by not applying pressure to one HEX side without either the opposite door bolted closed or suitable bracing installed on the open side. An annular gasket initially was selected which when placed in its groove provided a 1/16″ gap between the exchanger spiral surface and the door. At first, this gap was considered small enough so that any short-circuiting negligibly impacted performance, particularly the recuperator HR. Subsequently, the gap size was realized to be critical, especially for high aspect ratio ("pancake" type) HEXs like the recuperator. The smoothness and straightness of the spiral and door faces (tolerance of $\pm 1/32$″) also assured a consistent gap, minimizing bypassing, and maximizing heat transfer; HEXs were modified to be within this tolerance. Observed pressure drops during operation (150°C inlet retention loop temperature, 100 lpm water) approached design values for cases where this gap was minimized through installation of compressible gaskets. Both an annular gasket (Gylon 3510; Garlock Sealing Technologies, Palmyra, NY, USA) and a full-face gasket (Gylon 3545) were used to implement a full-face gasket installation with gasket material compressed so as to cut into the spiral face.

Low point drains were installed to permit complete system drainage with steam barriers applied to sterile process side drain valves to reduce sterility risk. These drains were fed by small "U" shaped notches in each wind of the spiral from the center down to the door drain. These notches were expected to negligibly impact performance relative to the gap. The extent that gaps or notches remained when a pliable, full-face gasket was installed was estimated by qualitative assessment of HEX gravity draining rates, which corresponded to measured pressure drops closer to design values. For the HEX gaskets selected, the remaining water after gravity drain was 20–50% of the entire HEX hold up volume, suggesting only very small gaps. This water was removed by subsequent blow-down using a 90 psig air supply.

A second cooling HEX was required for water sterilization conducted without a pressurized recirculation vessel. This HEX was cooled with chilled/cooling water and not by flashing, and it is referred to as a "flash" cooler throughout this paper. Since this pilot scale system was used intermittently, a sterilized system was not continuously maintained by recirculating sterile water between media runs, which often is done in production

facilities. This "flash" cooling HEX also was sized to directly replace the process cooling HEX. Since process coolers experienced the highest extent of thermal cycling, they were more likely than the other HEXs to fail based on previous experience. In addition, it was desirable to avoid using chlorine treatments to reduce bioburden in chilled and tower cooling water since this adversely affected stainless steel integrity [98]. Other causes of stress cracking and pitting corrosion during normal operations and cleanouts also existed [55], and their impact needed to be minimized.

Chilled/cooling water flowrates to cooling HEXs were sized for reasonable exit temperatures to minimize load on the chiller/cooling tower and reduce deposits that formed at higher outlet cooling water temperatures above 50°C [106]. The peak design condition was for water sterilization of the system and not production of sterile media. The observed rise in chilled water temperature was within design values when full cooling was applied but not when the control valve restricted flow to attain the desired outlet temperature set point (Table 6). Less water was used for cooling when under control than was assumed in the design since (1) process and "flash" coolers were oversized and (2) media outlet temperature and chilled water flowrate cannot both be specified.

Hot water heating loop

A hot water or tempered heating loop involves indirect heating without direct steam contact, and it utilizes a HEX, expansion tank, and circulation pump to heat water to above 150°C. It is more expensive than direct steam injection since additional equipment is required, but hot water loops have some key advantages.

Direct steam injection can be accomplished with a specialized steam water mixing valve, for example a Pick heater [79]. Although it is more energy efficient since heat up is almost instantaneous, its ability to provide accurate temperature control has been debated. It has a faster response time, can be used with solids-containing media, and is easier to clean and maintain [97], but it is sensitive to source steam pressure and media composition changes. Limited theoretical design information is established for these mixers, although detailed photographic examination of injected steam characteristics in water as a function of flow Reynolds number is available [77]. The key drawback to direct steam injection is process stream dilution, which can be up to 20 vol.% [83]. Excess water must be removed by subsequent flashing elsewhere in the system or the initial feed concentration must be adjusted. Also, since medium is exposed directly to steam, it may accumulate any additives or iron present in the steam [15]. Finally, there can be additional noise from direct steam injection into flowing liquid in some applications.

There is higher energy in steam (2,260 kJ/kg energy released from condensing steam) versus the heat capacity, C_p, of water of 4.2 kJ/kg K, making condensing steam heat content 540-fold higher than hot water heat content on a per degree basis [5]. In addition, injected steam heat transfer coefficients are 60-fold higher than indirect condensing steam heat transfer coefficients [77] and are not reduced by fouling as in a HEX [45]. Consequently, there are advantages of direct steam injection due its higher steam utilization efficiency [97] for high temperature sterilization of milk [82] and beer mash heating [5].

Based on its advantages for media sterilization, indirect heating via a hot water loop was implemented. A shell and tube 316 L stainless steel HEX was selected for this application since a spiral HEX was not found to be cost-effective for the size required. The hot water loop utility piping, originally carbon steel, exhibited substantial amounts of iron oxide corrosion due to its operation at higher temperatures. This build-up throughout the hot water loop was subsequently removed by a citric acid wash and piping was replaced by stainless steel. The hot water loop was designed for an operating temperature of up to 160°C and pressure of 75 psig using compressed air (>80 psig) applied to the expansion tank. Installation of a computer limit of 160°C for the loop temperature was necessary to avoid inadvertent system over-pressurization since the steam control valve opened fully during initial loop heat up.

Inlet retention loop temperature was controlled for these loops rather than outlet temperature, commonly used in pasteurization applications [82], owing to longer loop residence times for medium sterilization applications. Sterilization inlet temperature was controlled in either automatic or cascade mode. In automatic mode, a single loop was used to modulate hot water temperature to control retention loop inlet temperature at the outlet of the heater. In this single loop feedback control, wider periodic fluctuations have been found, but response time is quicker [27]. In cascade mode inlet temperature was used for primary control, and hot water temperature input was used as the secondary control loop. Using cascade control, the slave, inner or secondary loop manipulated the steam control valve to control water outlet temperature from the hot water HEX. The master, outer or primary loop manipulated the secondary (slave) loop set point to control medium outlet temperature on the final heating HEX prior to medium entry into the retention loop. This control has been found to be smoother and more accurate [91], but it has about a twofold longer response time [27]. Steam valve signals were more stable under cascade control with more constant steam flows instead of oscillating between high and low steam supply flow rates as in single loop control. An alternative feed forward control algorithm also has been used in other systems to anticipate process upsets due to load changes and to ensure tight control of product outlet temperature from the retention loop [56], but this strategy was not implemented in the current system.

The hot water loop temperature controllers initially were tuned using the Ziegler–Nichols closed loop

method [107] for both primary and secondary loops. Tuning constants for the secondary loop were first determined from the ultimate gain (specifically controller gain that causes continuous cycling) and ultimate period (specifically cycle period). Next, the primary loop was tuned with the secondary loop placed in cascade using these constants. The speed of the slave (secondary) loop was slowed down considerably and reset minimized [70] to gain more precise control (± 0.1°C) of inlet temperature in cascade mode. Together with low heat loss over the insulated retention loop, this tuning strategy permitted operation at more uniform sterilizing temperatures. Thus, sterilization temperature effects on subsequent production media performance were quantified more precisely, and operation with a safety factor of several degrees was avoided.

Retention loop

The retention loop (holding tube or box) was composed of thirty, 2″ diameter tubes (schedule 10 pipe with an ID of 2.16″ and wall thickness of 0.11″), each with only one weld over the 40 ft straight length, plus 29 connecting *U*-bends. These *U*-bends were fabricated from 2″ pipe bent by machine that resulted in a minimum thickness at the bend slightly less than normal schedule 10 pipe. The total length was 1,253 ft (382 m). The L/D was 9,318, suggesting that a narrow residence time distribution (and low axial dispersion) was achievable with sufficient turbulent flow. Also, additional mixing at each *U*-bend owing to its curvature might further reduce axial concentration gradients, although this effect has not been mentioned specifically in the literature.

The retention loop was designed to be drainable, and tubes were arranged in two banks in an ''accordion-type'' fashion on a 0.11 incline. Pipe supports were designed to permit expansion [96]. A high point vent valve was installed in the loop for draining and for bleeding of air during steaming/filling. (This vent valve did not appear to be required since a negligible amount of air exited the system when it was opened). Jumpers were configurable for variable retention loop volumes of 18 (540 L), 20 (600 L), 24 (720 L), 28 (840 L), or 30 (900 L) tubes. All of the jumpers were located on the same end of the retention loop with a removable insulation cover. Removable *U*-bends were attached using pipe-to-I-line ferrule fitting adaptors with minimal welds and maintaining the inner diameter so that flow was not constricted.

The retention loop was required to operate as close to isothermally (adiabatically) as possible. Improved insulation was installed by packing fiberglass blankets inside 2″ thick fiberglass board surrounding the faces between the frame and tubes. This method was preferred over insulating individual tubes since the large insulation thickness required around each tube adversely enlarged overall loop dimensions. The temperature profile along the length of the retention loop was assumed to be linear [35]. For this improved insulation, observed retention loop temperature drops as a function of flowrate compared favorably with design values.

Flow and pressure control

Flow and pressure control was composed of five loops that, although not related by software linkages, were closely related operationally. Two flow control valves were installed with one located after the centrifugal inlet feed pump and one after the centrifugal booster pump (Fig. 1a). The system was designed to utilize either a positive displacement (Moyno) or centrifugal inlet feed pump. When the positive displacement pump was used, both flow control valves were held fully open and flow was controlled using the Moyno pump's variable speed drive. When the centrifugal feed pump was used with the booster pump, booster pump suction pressure was controlled just prior to the booster pump suction and flow was controlled at the booster pump discharge only. (The flow control valve after the centrifugal feed pump was not used since this starved the booster pump suction).

Three pressure control valves also were installed. One pressure control valve, located on the recuperator inlet piping on the booster pump suction side, was set to maintain a positive pressure differential to avoid leakage on non-sterile feed should a HEX breach develop [sterile side at higher average pressure (0.8–1.5 kg_f/cm^2) than the non-sterile side]. The second and third valves were located after the process and ''flash'' coolers respectively (Fig. 1a) to maintain system pressure above the boiling point, which eliminated noise and potential damage from hammering [96]. To avoid leakage of non-sterile cooling fluids, the pressure on the utility side of the process cooler can be operated slightly below that of the sterile process side [96] by raising the system back-pressure or by reducing the chilled water supply pressure (i.e., by opening the supply to the nearby ''flash'' cooler).

Piping and HEX pressure drops were designed to be low so that sufficient back-pressures were attainable at the system outlet to provide adequate protection against flashing. There were limits to the range of suitable temperature and back-pressure combinations that avoided operating close to the fluid flashing point (Table 2). In addition, sufficient system flowrate (>40 lpm) was necessary to maintain back-pressure and flow consistency to avoid flashing.

The tuning strategy for the system began with tuning each flow and pressure loop individually and then operating them together, slowing down the response of the pressure loops as necessary to eliminate interactions. Loops were tuned using the Ziegler–Nichols method [107]; however the loop response with these settings excessively oscillated even before approaching set point. For flow and liquid pressure loops, large proportional bands (i.e., small gain) and fast reset action (i.e., small reset/integral time) are recommended [6]. Proportional and integral constants only are recommended for most

liquid flow control with only integral constants (i.e., floating control) recommended for noisy loops [64]. Consequently, gain and reset time were reduced so that integral control was the dominant action, which reduced oscillations. In addition, booster pump suction pressure control was deliberately detuned to have a slow response so as not to interact with flow and system back-pressure controllers (which themselves did not interact with each other). Thus, both booster pump flow and suction pressure controllers could be used together with no instability. Table 3 shows the tuning constants selected.

Switching valve station

The switching valve station was comprised of several diverter valves to direct the flow of steam, water, or medium to distribution, recycle, condensate trap, or system sewer as desired (Fig. 1b). The system switched according to the following valving arrangements (Fig. 1a, b): (1) system recycle to circulation tank (after passing through "flash" cooler; used for clean-in-place (CIP) and water sterilization), (2) transfer (feed) of sterilized medium to fermenters/waste tank, (3) system flow to sewer after process cooler, (4) system flow to sewer after "flash" cooler, (5) steam sterilization through process cooler to its condensate trap, and (6) steam sterilization through "flash" cooler to its condensate trap. Simultaneously with pathway switch, a steam barrier was applied to the pathway not being used to maintain sterility.

Isometric design of the switching station was challenging since several automatic valves with actuators were located in close proximity to reduce dead legs. Actuator size was minimized by sizing appropriately with little excess buffer for the facility instrument air pressure. Limit switches were avoided to save additional space as well as to streamline installation and maintenance costs.

Instrumentation

Sterilizer instrumentation is described in Table 4. In general, instrumentation mounting was important both for sanitary operation and for accurate instrument measurements. Remotely mounted transmitters were used where needed to extend temperature range suitability of instrument sensors (e.g., flowmeters) and where helpful for space and access reasons. Wherever possible, locally indicating transmitters were selected which permitted operation by a single person since the human/machine interface (HMI) was upstairs in the facility control room. Transmitters were mounted either in a panel (drawback of additional wiring but able to be factory tested) or on the skid (drawback of crowding skid access but avoids cost of a separate panel).

Accurate measurement of temperature was critical to ensuring that adequate medium sterilization was achieved and permitting reliable F_o and R_o calculations. Typical accuracies reported in HTST pasteurization equipment are ± 0.5°C at 72°C between indicating and

Table 3 Optimized tuning constants for sterilization of test media

Parameter	K_p	T_1 (min/repeat)	T_2 (min)
Flow control valve after centrifugal feed pump (40–100 lpm)	0.08	0.05	0
Pressure control valve on suction of booster pump			
40–60 lpm	0.05	0.30	0
80–100 lpm	0.05	0.20	0
Flow control valve after centrifugal booster pump (40–100 lpm)	0.045	0.05	0
Hot water temperature control of retention loop inlet—sterilization temperature of 135–150°C cleaning temperature of 60–80°C (40–100 lpm)			
Primary (outer)	0.36	0.5	0.225
Secondary (inner)	20.0	20.0	0.20
Pressure control after process cooler—Moyno or centrifugal inlet feed pump			
40–60 lpm	0.05	0.10	0
80–100 lpm	0.05	0.08	0
Pressure control after "flash" cooler—Moyno or centrifugal inlet feed pump			
40–60 lpm	0.05	0.10	0
80–100 lpm	0.05	0.08	0
Temperature control of process cooler cooling to 35°C	1.5	1.0	0.25
Temperature control of "flash" cooler-during sterilization cooling to 35°C and with 35°C inlet feed (40–100 lpm)	1.5	1.0	0.25
Temperature control of "flash" cooler-during cleaning solution cooling to 60°C and with 60°C inlet feed			
60 lpm	0.48	1.35	0.5
80–100 lpm	1.5	1.0	0.25

(1) Zero T_2 values were used for faster (relative to temperature loop) pressure and flow control loops. (2) Slightly different tuning constants required for (a) Moyno and centrifugal feed pumps and (b) 40–60 and 80–100 lpm flowrates to remain within desired ± 0.1 kg_f/cm^2 back-pressure variation. Tuning constants for 40–60 lpm worked up to 80 lpm. (3) At 60 lpm slower tuning required for "flash" cooler when cooling to 60°C for cleaning (inlet feed of 60°C) than cooling to 35°C (inlet feed of 35°C) during sterilization. (4) Higher T_2 value for primary hot water loop relative to its T_1 value minimized variations of slower secondary temperature control loop

Table 4 Instrumentation

Parameter	Model	Features
Temperature	Rosemount 3144PD1A1NAM5C2QPX3	0–200°C (hot water loop) 0–160°C (all others)
Flow	Micromotion R100S128NBBAEZZZZ	0–120 lpm
Pressure	Rosemount 3051CG4A22A1AS1B4M5QP	0–10 kg_f/cm^2 (feed and booster pumps) 0–6 kg_f/cm^2 (post-cooler HEXs)
Conductivity	Rosemount 225-07-56-99LC/54EC-02-09 Rosemount 403VP-12-21-36/54EC-02-09	0–100 MS/cm triclamp connection 0–100 μS/cm triclamp connection
Temperature control	Fisher-Rosemount 1052-V200-3610J	Software limit of 160°C for hot water loop
Flow control	Fisher-Rosemount 1052-V200-3610J	Flow control valves usable with either transmitter
Pressure control	Fisher-Rosemount 1052-V200-3610J	Software adjustment to prevent full closing of system back-pressure valve
Steam control	Fisher-Rosemount 667-EZ-3582	125 psig unregulated plant steam supply
I/P transducer	Marsh-Bellofram 966-710-101	3–15 psig compact
Solenoid	Asco series 541 multifunction ISO 1 mono stable	Spring-return piston actuators

recording temperature devices and ± 0.25°C at 72°C between test and indicating devices [92]. This compared favorably with the loop accuracy of ± 0.21°C for this system, estimated based on stated vendor accuracy for matched sensors [86].

Pressure loop accuracy was ± 0.02 kg_f/cm^2. The system back-pressure valve was capable of controlling pressure for flowrates ranging from 40 to 100 lpm using a computer-controlled maximum output of 80% closure to prevent unintentional shut off when operating with the positive displacement Moyno pump. In contrast, a closure of at least 95% was required when operating with the centrifugal pump since the pump output pressure was lower. A pressure and temperature gauge or transmitter was installed on the inlet and outlet of both sides of all HEXs for assuring adequate heat transfer performance and determining when HEXs required cleaning. These instruments also were important to evaluate individual unit performance for systems of interrelated HEXs during trouble-shooting [39].

Accurate measurement of volumetric flow was critical to ensuring that medium was properly sterilized for the appropriate residence time. A back-up flowmeter was installed for confirmation. Coriolis meters (Micromotion; Rosemount, Chanhassen, MN, USA), with a meter accuracy of ± 0.5% of flowrate (loop accuracy of ± 0.6% of flowrate), were selected rather than magnetic meters. Since flow measurements were based on fluid density, Coriolis meter readings were similar for both deionized and process (city) water ($< \pm 0.5$ lpm at 60–100 lpm) and within expected variations. Coriolis meters also were insensitive to media composition changes, specifically the switch from media to water, assuming these changes negligibly affected fluid density and were not affected by the hydraulics of medium to water switches. However, volumetric flow rate readings were up to 5.5% higher after the recuperator than before it owing to density decreases with temperature for specific medium types. [Mass flowrate (kg/min) readings were similar]. Finally, since air bubble entrainment altered density readings and thus Coriolis flowmeter readings, a variable speed agitator (5:1 turndown) was installed on the larger non-sterile medium feed tanks. For soluble media, shutting off the agitation also minimized air entrainment.

Proper Coriolis flowmeter installation was critical to performance. The preferred orientation was in a vertical upward flow section of pipe so that the flag filled and drained completely. Alternatives were not attractive: in the horizontal position pointing downwards the flag does not drain, in the horizontal position pointing upwards the flag incompletely fills due to air entrapment, and in the vertical position in a downward flow section of pipe the flag incompletely fills owing to gravity drainage. It also was necessary to secure the surrounding pipe to minimize interfering vibrations.

Conductivity sensors were used on-line to measure changes in the composition upon switching inlet feed stream contents and between inlet and outlet streams. One conductivity meter with a range of 0–100 μs/cm detected DIW with typical conductivities of 2.1 μs/cm during cleaning. Two other conductivity meters, each with a range of 0–100 Ms/cm, were located on feed (after the inlet feed pump) and outlet (after the process cooling HEX) of the sterilizer system (Fig. 1a). Similarly to the flowmeters, they were mounted in the vertical flow section to ensure no adverse effects on readings. Conductivity monitoring at the cooling water exit may enable instant detection of a cooling HEX breach [93], but this leak might have to be fairly substantial since cooling water and media conductivities are similar in magnitude.

Control system

Strategy

The control system strategy utilized minimal sequencing with manual operation preferred both to reduce installation expense and maximize flexibility. The system was composed of about 100 I/O (input/output) with about

55% analog input/output (AI/AO) and 45% digital input/output (DI/DO). The controls were interfaced to an existing Honeywell Total Distributed Control 2000/3000 hybrid system using newly-installed, dual (redundant) Honeywell High performance Process Manager controllers. Field-mounted (remote) I/O was installed inside a Nema 4× enclosure.

Calculated values by the control system

Several calculated values were displayed on the HMI to permit alarming and trending. These parameters included the temperature difference (inlet minus outlet) across the insulated retention loop, flowrate difference across the recuperator (upstream minus downstream), conductivity difference (inlet minus outlet), and pressure difference across the recuperator (outlet of hot side minus inlet of cold side). In addition, the totalized volumetric flowrate was calculated based on flowmeter readings rather than using the flow transmitter totalizer signal since implementation of the former was more straightforward.

Values of F_o and R_o were obtained based on on-line calculation of system residence time. The flowrate measured after the recuperator HEX was used in the calculation. Activation energies, E_a, of 16,800–26,000 cal/mol used for R_o generally were lower than those of the various spore types of 67,700–82,100 cal/mol used for F_o [34]. An E_a of 67,700 cal/mol was used for F_o [105] and an E_a of 20,748 cal/mol was used for R_o [17].

An adjustable filtering function [53] could be applied to final calculated F_o and R_o process variable values (PV) to smooth fluctuations caused by pulsations in flow and temperature readings. This function (Eq. 16) had only one user adjustable parameter for the filter value (FV):

$$\text{New PV} = \text{Old PV}\ (1 - \text{FV}) + \text{Measured PV}\ (\text{FV}). \tag{16}$$

With FV set to 1.0 (i.e., no filtering), variations of F_o and R_o were less than 1%. In addition, a user adjustable input permitted entry of proper retention loop volumes, V_s, to ensure accurate residence time, t_R, calculations.

Three methods were used to evaluate this on-line calculation for a simulated continuous sterilization run (Table 5): (a) calculation for 1 min residence time intervals along the loop length and summation of values over the entire length of pipe, (b) use of the average of retention loop inlet and outlet temperatures in the calculation, and (c) averaging of two separate calculations using inlet and outlet temperatures. Although method *a* was most accurate, method *b* was selected since the error was sufficiently small, and implementation was more straightforward. In general, errors were smaller for R_o than F_o. This approach was in contrast to the dairy industry where a worst case lethality has been calculated using the outlet temperature of the insulated retention loop [91].

Tuning constants and control variation

For all control loops, proportional/integral/derivative (PID) control in the fast mode (PID calculation updated every 0.25 s) was utilized based on three parameters (definitions are specific to the Honeywell control system): the proportional gain, K_P, unitless (reciprocal of the proportional band); the integral constant, T_1, min per repeat; and the derivative constant, T_2, min. Control tuning constants were developed for water (Table 3) then tested and found to be acceptable for different media (55 wt.% cerelose, 50 vol.% glycerol). Slightly different values were optimal for flowrates of 40–60 lpm than for 80–100 lpm with lower flowrate range constants performing somewhat better than higher flowrate range constants between 60 and 80 lpm. Variations in these control loops, characterized under various operating conditions, were found to be acceptable. Hot water loop control performance did not change significantly with media type since system disturbances expected for media were likely to be dampened relative to water.

System performance

Water and media testing

The three types of media tested were water [both deionized (DIW) and process (city)], 55 wt.% cerelose and 50 vol.% glycerol. Heating of non-sterile feed tanks by external jacket platecoils and recycling of cooled effluent back to the system inlet permitted system testing with feeds of differing temperatures over the range of 15–60°C. ''Once-through'' testing was used only for cerelose to reduce Maillard reactions, which were feared to soil sterilizer internals. Water and glycerol were recycled by setting the ''flash'' cooler temperature to the desired inlet temperature, permitting testing of process cooler performance at or above inlet feed temperatures. The manner in which readings were taken affected assessment of their variability; readings were observed for a few seconds, then a mental average was taken and evaluated to determine whether the bounce was within reasonable limits. Computer system historical trends, which recorded data every 1 min also were used to assess variability.

Pressure drops were calculated for each HEX for various media considering the temperature effect on the inlet feed stream density. The vendor's proprietary software was used which did not account for gaps between spiral face and HEX door and assumed a tighter-than-actual stud spacing. Thus, the design HEX pressure drop was likely overestimated. Re-calculation (data not shown) using published equations for the pressure drop across the spiral HEX [71], which also did not account for the gap impact, resulted in estimates somewhat closer to measured values. The retention loop pressure drop was calculated using a retention loop

Table 5 Comparison of calculation methods for F_o and R_o for a simulated continuous sterilization run with a 2°C temperature drop across the insulated retention loop and $t_R = 10$ min (error calculated relative to method a)

	Method	F_o (min)	Error (%)	R_o (min)	Error (%)
a	Integrate at 1 min residence time intervals	439.93	Basis	31.84	Basis
b	Use average of inlet and outlet loop temperatures	437.00	0.67	31.82	0.06
c	Average separate calculations using inlet and outlet loop temperatures	445.62	1.30	31.88	0.13

equivalent length of 1,525 ft (including elbows and pipe-to-tube adapters) and f values according to Table 9.

Calculated pressure drops were compared to measured values (data not shown). For the 100 lpm flowrate, most measured values were about 30–40% lower than calculated values with the exception of the heater's cold side which was 2.5- to 3.5-fold higher. For the 40 lpm flowrate, observed values were substantially higher (6.5- to 10-fold) than calculated values for the heater's cold side. These results may indicate difficulty in predicting pressure drops for the lower aspect ratio heater HEX (Table 1), particularly at its higher operating temperatures relative to the other HEXs. Measured pressure drops for various test media were reasonably similar.

System temperatures were calculated for each media type and compared with observed values (Tables 6, 7, 8). Design HR, NTU, and TE were calculated assuming no temperature drop across the retention loop (i.e., retention loop inlet temperature equal to hot side recuperator inlet temperature). Negligible heat loss for the retention loop, HEXs, and piping also was assumed; design values would be higher if these losses were included.

Observed temperature profiles, HRs, NTUs, and TEs generally met or were somewhat lower than design depending upon which design basis was utilized. The primary factor causing under-performance was believed to be lack of allowance for the gap that was likely present even with pliable, full-face gaskets installed owing to unavoidable variations in flatness of the HEX spiral and door faces. The observed hot side recuperator inlet temperature from the non-adiabatic retention loop was lower than the isothermal design assumption and thus raised measured values compared with design HR, NTU, and TE. Viscosity decreases with higher temperature resulted in improved performance.

System draining hold up volume

The system's hold up volume was established by running process water into a completely drained and air-blown system. It was determined when water reached a certain section by opening the adjacent downstream drain valve. Measured hold up volumes agreed with calculated ones within reasonable limits but may have been affected by the ability to fill the system completely at the lower flowrates used to obtain these measurements. Overall, the impact on design residence times of these differences was negligible, however.

Inlet feed stream and outlet distribution stream switching

Prior to testing all instrument air connections to the switching skid were checked for leaks and proper venting. When switching to the distribution manifold (sterilizer feed to fermenters) from either the sewer or recycle flow paths, transient flow and pressure spikes and their effect on inlet and outlet retention loop temperatures were observed and found to be negligible. When sterilizer distribution was switched from the receiving waste tank to the desired fermenter vessels, pressure spikes also had a negligible effect on temperature. Minimal disturbances were observed for actual water-to-media switch over when the system feed was changed from water to 55 wt.% cerelose and back again. In all of these instances, an acceptable temperature spike was considered to be less than the variation observed during normal flow operation. Since these spikes were negligible, it was not necessary to flush the system appreciably after a switch to regain steady performance. In addition, sewer to recycle, waste to sewer, and fermenter to waste transitions were not potential sterility risks since these typically occurred after sterilized medium transfer was completed.

Heat losses

For this system, the target retention loop temperature drops (Table 2) were met or exceeded for the test media at residence times of 9–22.5 min. In another study, for a retention loop of 50 mm (2″) diameter, the temperature drop was negligible for short residence times of 4 s (hold temperature of 85°C and room temperature of 20°C) regardless of whether the retention loop was insulated (0.005°C) or not insulated (0.04°C) [55]. For longer residence periods of 40 s, the temperature drop was 0.04°C for insulated and 0.35°C for non-insulated cases. These temperature drops are expected to increase with higher residence times and higher holding temperatures. Extrapolating from these data assuming operation at 85°C, a change of 0.0583°C/min was expected, translating to an expected drop of 0.525°C for a residence time of 9 min. Since the actual operating temperature was substantially higher at 150°C, the

Table 6 System performance using water at 100 lpm (900 L retention volume unless noted otherwise)

Parameter	Feed inlet of 15°C		Feed inlet of 25°C	Feed inlet of 60°C		
	Design	Observed Moyno/centrifugal	Design	Design	Observed Moyno/centrifugal	Observed Moyno 540 L
Recuperator cold side inlet feed (°C)	15.0	15/15	25.0	60.0	59/59	60
Recuperator cold side outlet/heater hot side inlet (°C)	120.0 (**126.0**)	120/120	122.5 (**128.0**)	131.0 (**135.0**)	131/132	131
Heater hot side outlet/retention loop inlet (°C)	150.0	150.1/150.0	150.0	150.0	150.0/150.0	150.01
Retention loop outlet/recuperator hot side inlet (°C)	150.0	149.2/149.1	150.0	150.0	149.2/149.1	149.02
Recuperator hot side outlet/process cooler hot side inlet (°C)	45.7 (**39.6**)	46/43	53.2 (**47.6**)	79.5 (**75.4**)	80/78	77
Process cooler hot side outlet (°C)	35.0	35.0/35.0	35.0	35.0	35.0/35.1	34.8
Process cooler cold side inlet (°C)	6.0	8.6/8.2	6.0	6.0	8.3/N/A	N/A
Process cooler cold side outlet (°C)	12.0 (**8.5**)	41/50	12.0 (**11.6**)	12.0 (**11.4**)	49/N/A	N/A
Recuperator heat recovery (HR, %) (Eq. 14)	77.8 (**82.2**)	77.7/77.8	78.0 (**82.4**)	78.9 (**83.3**)	79.1/80.2	78.9
Recuperator NTUs (Eq. 12)	3.46 (**4.57**)	3.49/3.68	3.50 (**4.62**)	3.69 (**4.93**)	3.68/4.05	4.06
Recuperator thermal efficiency (TE) (Eq. 13)	3.50 (**4.63**)	3.60/3.61	3.55 (**4.68**)	3.74 (**5.00**)	3.96/4.27	3.94

(1) Water not tested at 25°C but design is included for comparison. (2) Process cooler inlet temperature reading taken from building chilled water supply temperature. (3) Design numbers calculated based on intermediate temperatures needed to reach 150°C at the retention loop inlet assuming that most of the load was undertaken by the heating HEX based on a maximum heating loop temperature of 160°C. Thus, less than the maximum area of the recuperator was utilized in some cases. (4) Design numbers in bold calculated based on 100% utilization of the recuperator surface area and permitting the hot water loop to operate at values less than 160°C

Table 7 System performance (900 L retention loop volume) using 55 wt.% cerelose at 65 (25°C inlet temperature) and 100 lpm (60°C inlet temperature)

Parameter	Feed inlet of 25°C			Feed inlet of 60°C		
	Design	Observed Moyno/centrifugal		Design	Observed Moyno	
	65 lpm	65 lpm	40 lpm	100 lpm	100 lpm	40 lpm
Recuperator cold side inlet feed (°C)	25.0	25	25/26	60.0	57	60
Recuperator cold side outlet/heater hot side inlet (°C)	105.0 (**110.5**)	120	126/125	128.0 (**127.0**)	127	130
Heater hot side outlet/retention loop inlet (°C)	150.0	150.0	150.0/150.0	150.0	150.0	150.0
Retention loop outlet/recuperator hot side inlet (°C)	150.0	148.8	148.1/147.9	150.0	149.1	148.1
Recuperator hot side outlet/process cooler hot side inlet (°C)	77.2 (**64.5**)	54	47/51	85.2 (**86.3**)	82	77
Process cooler hot side outlet (°C)	35.0	35.7	35.1/34.3	35.0	35.0	35.8
Process cooler cold side inlet (°C)	6.0	8.2	7.5/NA	6.0	7.7 (est)	7.7
Process cooler cold side outlet (°C)	12.0 (**13.3**)	40	42/NA	12.0 (**21.1**)	61.4 (est)	45
Recuperator heat recovery (HR, %) (Eq. 14)	64.0 (**68.4**)	76.0	80.8/79.8	75.5 (**74.4**)	75.3	77.8
Recuperator NTUs (Eq. 12)	1.65 (**2.17**)	3.29	4.58/4.13	2.89 (**2.72**)	2.98	3.99
Recuperator thermal efficiency (TE) (Eq. 13)	1.78 (**2.17**)	3.30	4.57/4.32	3.09 (**2.91**)	3.17	3.86

(1) *Est* estimation by using data for 40 lpm case as a basis. (2) Cerelose after sterilization was dark brown at 150°C; lighter brown at 135°C. (3) At 25°C, 55 wt.% cerelose forms a cloudy dispersion in feed tank with entrained air (requiring several minutes to dissipate after agitation is stopped) compared to 55 wt.% cerelose at 60°C where solution in feed tank is clear. (4) Design numbers in bold (see note 4 of Table 6) for 65 lpm interpolated from 60 and 80 lpm cases

observed drop of 1°C appears consistent with these earlier studies.

Infrared pictures (Inframetrics model PM250 Thermocam; Flir, Boston, MA, USA) of the retention loop and HEXs were taken to evaluate retention loop insulation effectiveness (particularly the removable jumper end) and HEXs heat losses due to lack of insulation. (Radiant heat loss due to thermal radiation was considered negligible). These pictures showed that the retention loop was adequately insulated. Typical HEX surface temperatures were consistent with the temperature profile of Table 6. Since cold fluids enter the HEX on the periphery and hot fluids enter in the center, there was minimal heat loss to the surroundings [100]. In addition, during water sterilization temperature drops were measured for the recuperator's hot media side (with the inlet cold side bypassed) and the process side of the process cooler (without chilled/cooling water flow). These drops were <0.3°C for the recuperator (aspect ratio of 3.5) and about 2.0°C for the process cooler (aspect ratio of 2.9). Lower heat losses were expected for thicker, lower aspect ratio HEXs and HEXs with more turns [99]. In addition, full-face gaskets minimized heat transfer rates to the HEX cover faces, which reduced heat loss.

System sensitivity

Variations in inlet retention loop temperature (± 0.05°C), system flowrate (Moyno feed pump- ± 0.015 lpm, centrifugal feed pump- ± 1.0 lpm), and back-pressure (± 0.05 kg_f/cm^2) generally were negligible across the operating range and for the various test media. As expected, flowrate variations were somewhat greater for the centrifugal than for the positive displacement Moyno feed pump. The relative sensitivities of retention loop inlet and outlet temperatures to changes in system back-pressure were found to be negligible. This behavior was improved from the prior direct steam injection design since steam/water mixing was more volatile and pressure-sensitive.

F_o and R_o

For a hold temperature of 150°C, F_o magnitudes were acceptable ranging from 3,000 min at 100 lpm to 6,500–7,000 min at 40 lpm. At 135°C, F_o was substantially lower at 150 min, but still representing a 50-log reduction for spores with a D value of 3.0 min. For a hold temperature of 150°C, R_o magnitudes ranged from 50 to 55 min at 100 lpm to 125–130 min at 40 lpm; at 135°C, R_o was substantially lower at 20 min. Acceptability of these R_o values depends on the degree and impact of media degradation for the specific process.

Reproducibility was high at $<1.5\%$ for the same inlet feed pump. F_o and R_o differences were $<10\%$ between the two inlet feed pumps using the same medium type, residence time, and sterilization hold temperature; these differences were presumed due to small volumetric flowrate changes, thus slightly altering residence times. Different flowmeters controlled flowrate depending on the inlet pump utilized, but the flowmeter after the recuperator was used for the calculation regardless.

Dimensionless groups and axial dispersion

For the retention loop, N_{Re} and N_{Bs} were calculated for each type of media at various system flowrates and at a sterilization temperature of 150°C (Table 9), starting with velocity estimation. Process bulk velocities for the retention loop, as well as HEXs, ranged from

Table 8 System performance (900 L retention loop volume) using 50 vol.% glycerol at 88 lpm using flowmeter after inlet feed pump (15°C inlet temperature) and 91.5 lpm (60°C inlet temperature)

Parameter	Feed inlet of 15°C			Feed inlet of 60°C		
	Design	Observed Moyno		Design	Observed Moyno/centrifugal	
	88 lpm	88 lpm	40 lpm	91.5 lpm	91.5 lpm	40 lpm
Recuperator cold side inlet feed (°C)	15.0	15	15	60	60/60	60/60
Recuperator cold side outlet/heater hot side inlet (°C)	125.8 (**116.0**)	114	117	131.0 (**128.3**)	128/128	130/130
Heater hot side outlet/retention loop inlet (°C)	150.0	150.0	150.0	150.0	150.0/150.0	150.0/150.0
Retention loop outlet/recuperator hot side inlet (°C)	150.0	149.1	147.9	150.0	149.1/148.9	147.9/148.1
Recuperator hot side outlet/process cooler hot side inlet (°C)	45.0 (**49.0**)	52	48	82 (**81.7**)	82/80	76/76
Process cooler hot side outlet (°C)	35.0	34.9	34.6	35.0	35.0 (est)/60.2	62.44/60.2
Process cooler cold side inlet (°C)	6.0	8.1	7.66	6.0	7.8/7.89	7.6/7.83
Process cooler cold side outlet (°C)	12.0 (**17.6**)	38.5	43.0	12.0 (**13.9**)	45.2 (est)/73	78/72
Recuperator heat recovery (HR, %) (Eq. 14)	82.1 (**74.8**)	73.3	75.6	78.9 (**75.9**)	75.6/75.6	77.8/77.8
Recuperator NTUs (Eq. 12)	4.10 (**2.97**)	2.75	3.19	3.47 (**3.16**)	3.16/3.32	4.14/4.11
Recuperator thermal effectiveness (TE) (Eq. 13)	4.58 (**2.97**)	2.82	3.30	3.74 (**3.16**)	3.23/3.25	3.92/3.87

(1) Glycerol at 60°C inlet feed temperature cooled to 60°C outlet temperature. (2) *Est* estimation by back calculating heat transfer coefficient for cooling using tower water performance data for similar test media/conditions. Chilled water flowrate varies, which alters heat coefficient, which changes chilled water outlet temperature. Chilled water flowrate and outlet temperature solved iteratively by balancing heat transferred (U A ΔT_{ln}) with heat absorbed (Q_M C_p ΔT). (3) Design numbers in bold (see note 4 of Table 6) for 88 and 91.5 lpm interpolated from 80 and 100 lpm cases

0.62–1.33 m/s at 100 lpm and 0.24–0.47 m/s at 40 lpm (Table 10). The velocity at 40 lpm was 40% of the value for 100 lpm. Over the 50 wt.% cerelose feed temperature range of 25–60°C and the water/50 vol.% glycerol feed temperature range of 15–60°C, there was only a very slight change in calculated velocity (data not shown).

Calculated system velocities were compared to expected settling velocity for a solids-containing media such as 5% cottonseed flour (Pharmamedia, Traders Protein; Memphis, TN, USA). According to the manufacturer, 91% of the particles are <74 μ. (i.e., pass through a 200 mesh screen) and particle density, ρ_p, is 1,485 kg/m^3. The particle settling velocity at 150°C based on a specific gravity of 1,013 kg/m^3 for a 50 g/L solution at 25°C (measured using a Fisherbrand, Category No. 11-555G hydrometer) was estimated at 0.016 m/s for 200 μ particles, 0.0054 m/s for 100 μ particles, and 0.0016 for 50 μ particles. These values were 15- to 100-fold lower (depending on the particle size assumed) than the lowest system velocities. Settling velocities were expected to be even lower as the temperature decreased owing to the higher specific gravity of water.

N_{Re} ranged from 53,000–150,000 regardless of media type (Table 9). Equation 11a was used to obtain f values ranging from 0.0204 to 0.0232 regardless of media type or flowrate, resulting in D_z values (Eq. 10) ranging from 0.0089 to 0.0235 over the flowrate range from 40 to 100 lpm. N_{Bs} values ranged from 17,150 to 18,300 and were relatively insensitive to either medium type or

Table 9 Key calculated parameters for the retention loop for an inlet feed temperature of 15°C, sterilization hold temperature of 150°C, and process cooler set point of 35°C (L/D of 9,318 for 900 L retention loop volume)

Parameter	Water (40–100 lpm)	55 wt.% cerelose (40–65–100 lpm)	50 vol.% glycerol (40–88–100 lpm)
N_{Re}	84,000–210,000	53,000–86,000–132,000	60,600–133,300–151,500
V (m/s)	0.305–0.762	0.335–0.518–0.823	0.335–0.701–0.792
f (Eq. 11a)	0.0222–0.0204	0.0232–0.0221–0.0213	0.0231–0.0212–0.0209
$D_z/VD = 3.57f^{0.5}$ [61], Eq. 10	0.532–0.510	0.544–0.531–0.521	0.543–0.520–0.516
D_z (m^2/s)	0.00890–0.0213	0.0100–0.0151–0.0235	0.00999–0.0200–0.0224
N_{Bs} (VL/D_z)	17550–18300	17150–17550–17900	17150–17950–18100
Water			
D_z/VD correlation [61]	0.33 ($N_{Re} = 10^4$)–0.2 ($N_{Re} = 10^5$)		
D_z (m^2/s)	0.00550 ($N_{Re} = 10^4$)–0.00837 ($N_{Re} = 10^5$)		
N_{Bs} (VL/D_z)	28350 ($N_{Re} = 10^4$)–46600 ($N_{Re} = 10^5$)		

(1) Surface roughness assumed to be equivalent to commercial steel ($\varepsilon = 4.57\times10^{-5}$ m, $D = 0.0549$ m, $\varepsilon/D = 0.00083$) [78]. (2). Inlet temperature variation from 15 to 60°C only slightly affects N_{Re} ($<1\%$) based on density change of volumetric inlet flow rate. (3) N_{Bs} for 540 L retention loop volume is about 60% of that for 900 L retention loop volume

Table 10 Calculated bulk velocities of HEXs for various test media (based on 40–100 lpm process flowrate, sterilization temperature of 150°C, process cooler set point of 35°C)

HEX	Process side velocity (m/s)			Utility side velocity (m/s)
	Water (15°C inlet feed)	55.0 wt.% cerelose (25°C inlet feed)	50 vol.% glycerol (15°C inlet feed)	
Interconnecting piping	0.47–1.26	0.47–1.33	0.47–1.32	N/A
Recuperator (both sides)	0.35–0.94	0.34–0.94	0.34–0.98	N/A
Heater	0.24–0.62	0.25–0.66	0.25–0.67	2.0
Retention loop	0.31–0.77	0.32–0.81	0.32–0.80	N/A
Process and "flash" coolers	0.35–0.87	0.35–0.89	0.35–0.88	3.3

flowrate (Table 9). Using the experimental correlation and applying it to water [61], N_{Bs} values were somewhat higher than the calculated values (Table 9), but reasonable considering the data scatter of the correlation itself. Thus, $N_{Bs} >> 1$ for expected operational ranges.

Dips for disturbances were shallower for the retention loop outlet than for the inlet and were observed about t_R minutes later. For example, at 100 lpm, an inlet temperature dip to 143°C (from 150°C) resulted in an outlet temperature dip to only 145.5°C. Based on the 1°C steady-state temperature loss observed, an outlet temperature dip to 142°C was expected, but not realized most likely due to axial dispersion.

Direct qualitative examination of axial dispersion was accomplished using step change and spike tests for flowrates of 40 and 100 lpm. For the step change test, water flowed through the sterilizer then the step change was performed quickly by switching from one feed tank at ambient temperature to a second tank at a higher temperature (60°C). The system was not heated and was operated without backpressure. For the spike (delta or pulse) change, a temperature spike in the hot water loop was created by quickly opening the steam valve fully and then returning it to its original output setting, taking care to maintain the peak temperature below 150°C. For both types of tests the non-sterile side of the recuperator was by-passed to avoid heat transfer, as well as reducing the piping length/volume (relative to that of the retention loop) between the switching point and the retention loop entrance (about 50 ft excluding spiral loops vs. 1,253 ft, 65 L vs. 900 L). It was difficult operationally to perform step and spike changes with sufficient rapidity owing to this hold up. The dispersion results are shown in Fig. 3a and b. Clearly the degree of dispersion increased at the lower flowrate of 40 lpm (versus 100 lpm) for both types of tests. However, the absolute value of the dispersion coefficient suggested by these data appears artificially higher than that predicted from the calculations.

Steam-in-place testing

The use of biological indicators (BIs) and thermocouples (TCs) was avoided in steam-in-place (SIP) testing since (1) fittings had to withstand higher pressures up to 10 kg_f/cm^2 and (2) the system was physically large precluding use of TCs with attached wires [although Valprobe (GE Kaye Instruments Inc., North Billericia, MA, USA) wireless TCs were one alternative considered]. TCs commonly have been used in pasteurization applications with a lower hold temperature of 72°C [82] and correspondingly lower pressure. BIs (in the form of feed inoculated with indicator organisms) were not considered desirable for contact with production equipment for pasteurization [47], although studies are underway to determine if non-indicator organisms can be used [82]. Simulations have been conducted (1) using laboratory or pilot scale test apparatuses with inoculated spore solutions, (2) by tracking an indicator enzyme [69] and/or (3) utilizing rigorous temperature distribution monitoring on laboratory and production equipment, obtaining spore inactivation kinetic data in parallel, then developing models to estimate lethality [47, 82, 92]. Installation of several temperature and pressure indicators for in process monitoring, along with a functional sterility test, was the preferred approach to demonstrate proper operation.

Operational testing was performed to test both the steam sterilization-to-water transition and water sterilization modes. Regardless of the sterilization method used, prior steam sterilization of the empty system and subsequent switching back pressure control from the "flash" to process cooler was required. Each method had key points requiring extra care- the initial water introduction for the steam sterilization-to-water transition and placing the empty non-sterile side of the recuperator on-line for the water sterilization. Thus, the time and attention required to execute either method was reasonably equivalent.

Using the steam sterilization-to-water transition and a 9 min residence time, three sterility tests employing soluble medium were successfully completed at 150°C and one at 135°C to test the F_o range of 150–3,000 min. One sterility test was successfully completed using the water sterilization method. Changes between non-sterilized and sterilized sterility medium were minimal for total dissolved solids ($< \pm 3$–8%) and conductivity ($< 3\%$ decrease), confirming minimal medium dilution since all heating was done indirectly. Glucose concentration (measured enzymatically by a YSI analyzer, Yellow Springs, OH, USA) decreased by 15–25%, likely reflecting glucose complexing with nitrogen during sterilization and not medium dilution. Further tests for different media (50 vol.% glycerol,

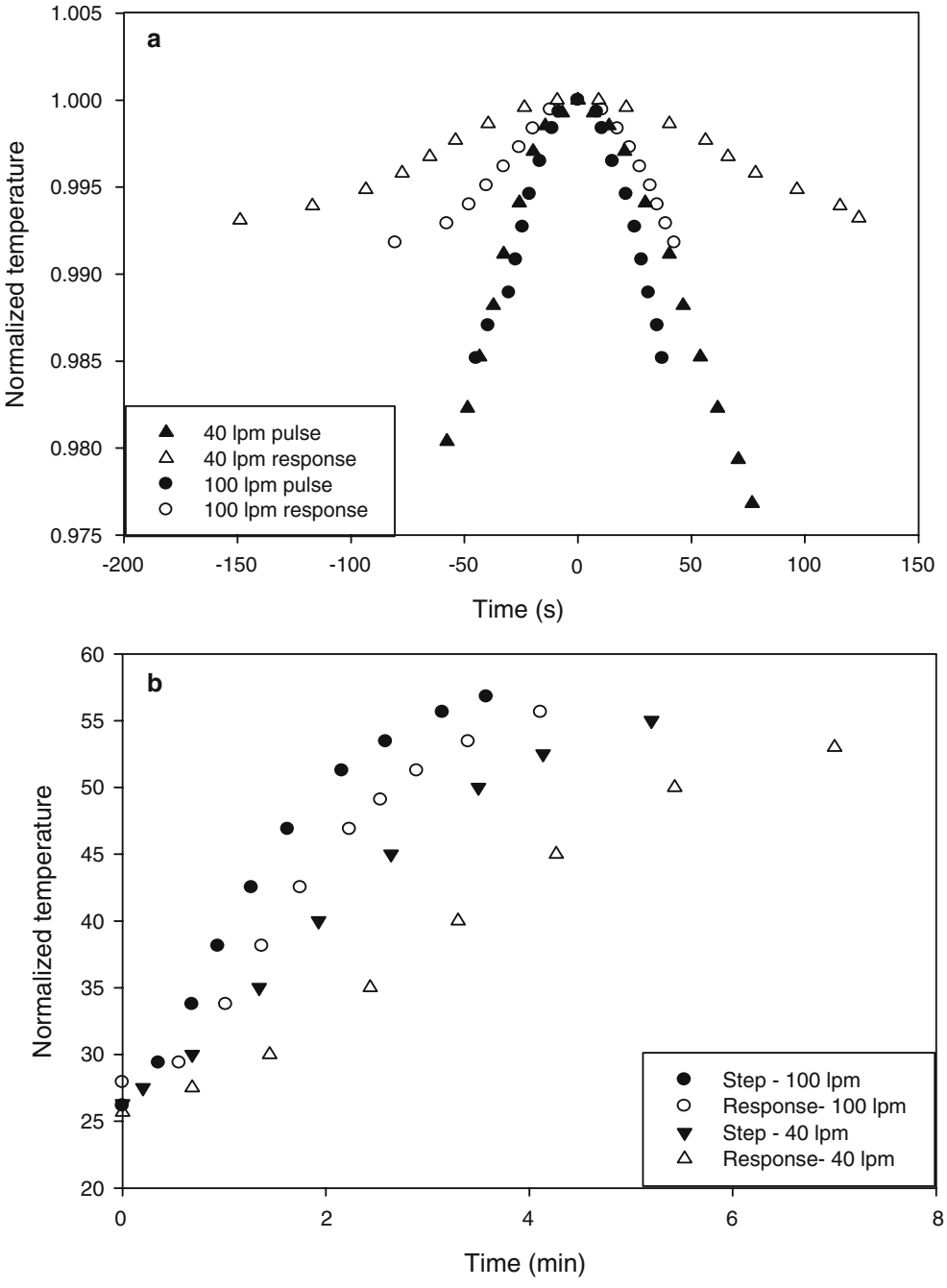

Fig. 3 Axial dispersion. **a** pulse, **b** step change

50 wt.% cerelose, 5 wt.% Pharmamedia) are to be done as process development requirements dictate.

Clean-in-place (CIP) testing

Cleaning of HEXs to remove fouling and solid accumulations was required both to maintain heat transfer performance and avoid system sterilization problems. After medium was run through the sterilizer, the system was flushed with water while at sterilization temperature for at least one system volume, then flushing was continued as the system cooled. An alkaline cleaning agent (typically 1.5 vol.% low heat #3; Oakite Products, Bardonia, NY, USA) was added to dissolve medium components as well as any denatured proteins. Besides alkaline cleaning agents, acid cleaning agents (typically 1.2 wt.% sulfamic acid) were used to dissolve mineral deposits. Also, a high pressure water stream (1,800–2,500 psi pressure) can be used to clean the spiral HEX channels [19, 71], although this required opening HEXs doors which was costly on a routine basis. The system was heated to 60–80°C, rather than sterilization temperatures of 135–150°C, which past experience indicated to be sufficient for cleaning. An additional set of tuning constants was implemented for these lower cleaning

temperatures (Table 3), but overall control was not required to be as tight as during sterilization.

Contact of the cleaning solution with all internal wetted sterilizer parts at a minimum required velocity of 1.5 m/s (2.0 m/s recommended) [24] was desirable. Although these high velocities were not achievable in the process side (Table 10), system cleanability was acceptable. There were significant concerns about cleaning HEXs with full-face gaskets installed due to the potential for accumulated residue where the spirals contacted the door and underneath the gasket at the center nozzles since the gasket hole was braced only by the spiral face. System cleanliness was evaluated by (1) examining inlet and outlet conductivity differences and comparing values to those for DIW, (2) analyzing rinse water samples for total solids, filtered solids, color, and ultraviolet absorbance, and (3) visual inspection and swabbing internal surfaces for total organic carbon (TOC), including the HEXs. There were no appreciable differences between source and rinse water in these measurements. Residue accumulation was negligible on the process sides of all spiral HEXs, and swab-testing results were less than 25 ppm TOC for each location examined.

Cleaning approaches utilized in the dairy industry for continuous pasteurization applications are consistent with the above approach. After processing in certain milk pasteurization applications, systems are rinsed with cold water, flushed with 1.5–2 w/v.% caustic detergent at 85°C for 30 min, cooled, drained, then flushed with water a second time [40]. For other dairy applications, the nature of the soil was primarily protein, butter-fat, and minerals [38]. In this latter case, an acid detergent first dissolved minerals and loosened burned on accumulation, which increased soil solubility in subsequent caustic detergent solution. Instead of draining and rinsing the system between detergent switches, caustic has been added directly to the acid solution to minimize energy costs associated with a second heating of the cleaning solution [38]. However, this short cut can result in soil particles already dissolved in acid or caustic solution potentially re-depositing on system surfaces as the pH changes.

Conclusion

Improvements implemented for a next generation, pilot-scale continuous sterilization system span the design, fabrication, and testing project phases and have been described. Advantages and disadvantages of various system features were evaluated based on literature analysis from fermentation as well as other related applications. Successful realization of these requirements depended on the adoption of an effective project strategy. The selected system vendor had experience primarily with the food industry since there were few new media sterilizers for manufacturing being constructed and even fewer for pilot plant process development use. Thus, it was critical to devote sufficient time to comprehensively determining system requirements. Development of a detailed sequence of operation as the piping and instrument diagram (P&ID) itself was developed ensured alignment of performance expectations. In addition, selection of a system (as well as HEX) vendor who was located nearby facilitated interim progress examinations prior to delivery.

The ''worst case'' design scenarios were determined carefully, ensuring that they did not create unnecessary additional costs. Agreement on the design assumptions and performance requirements was critical, particularly for calculated quantities. Specifically, the entire system operation needed to be evaluated when developing the HEX performance requirements. Interim temperatures and pressures were estimated based on the system's flow connections and not simply considering each HEX separately. Since the temperature rise in each HEX stream depended on actual flowrate, design calculations were done using expected flowrates and not solely the maximum flowrates that the HEX can support. Finally, a check of calculations for the various design cases ensured they were internally consistent.

Performance testing was devised to quantify actual operation versus design expectations. Intermediate pressure and temperature measurements within the system were compared to design calculations to identify performance issues. Communication of acceptable variability to the control and instrument system designer upfront ensured proper test criteria were met and steady state variations were acceptable. Tests were performed and documented for all operational phases. These system tests were considered critical to effectively characterizing the system's capabilities prior to placing the equipment in service.

Acknowledgments The following groups were involved in the design, construction, start up and qualification of this project: Merck Central Engineering (project management and construction management), Merck Automation Technology (instrumentation and computer system design), Aker-Kvaerner Engineering (K. Chauhan and P. Kardos, conceptual, basis of design, and detailed design), Honeywell (system integrator), APV Solutions (skid design and fabricator), Alfa-Laval (spiral HEX design and fabricator), Merck Research Laboratories Pilot Facilities/Quality Engineering and Fermentation Development and Operations departments.

References

1. Adams JP, Simunovic J, Smith KL (1984) Temperature histories in a UHT indirect heat exchanger. J Food Sci 49:273–277
2. Aiba S, Sonoyama T (1965) Residence time distribution of a microbial suspension in a straight pipe. J Ferment Technol 43(8):534–539
3. Aiba S, Humphrey AE, Millis NF (1965) Biochemical engineering. Academic Press, NY
4. Albert I, Mafart P (2005) A modified Weibull model for bacterial inactivation. Int J Food Microbiol 100:197–211
5. Alvarez E, Correa JM, Navaza JM, Riverol C (2000) Injection of steam into the mashing process as alternative method for the temperature control and low-cost of production. J Food Eng 43:193–196

6. Anderson GD (1983) Initial controller settings to use at plant startup. Chem Eng 90:116
7. Anonymous (1977) Spiral exchangers for continuous sterilization. Processing 23:19, 23
8. Armenante PM, Leskowicz MA (1990) Design of continuous sterilization systems for fermentation media containing suspended solids. Biotechnol Prog 6:292–306
9. Armenante PM, Li YS (1993) Complete design analysis of a continuous sterilizer for fermentation media containing suspended solids. Biotechnol Bioeng 41:900–913
10. Ashley MHJ (1982) Continuous sterilization of media. The Chem Eng 377:54–58
11. Ashley MHJ, Mooyman JG (1982) Design optimization of continuous sterilizers. Biotechnol Bioeng 24:1547–1553
12. Aunstrup K, Andressen O, Falch FA, Nielson TK (1979) In: Peppler H (ed) Microbial technology, 2nd edn, vol 1. Academic Press, NY, pp 281–309
13. Bailey K (1994) Understand spiral heat exchangers. Chem Eng Prog 90(5):59–63
14. Bennett CO, Myers JE (1982) Momentum, heat, and mass transfer, 3rd edn. McGraw-Hill Inc, NY
15. Blakebrough N (1968) Preservation of biological materials especially by heat treatment, Chap 12. In: Blakebrough N (ed) Biochemical and biological engineering science, vol 2. Academic Press, NY, pp29–63
16. Blake MR, Weimer BC, McMahon DJ, Savello PA (1995) Sensory and microbial quality of milk processed for extended shelf life by direct steam injection. J Food Prot 58(9):1007–1013
17. Boeck LD, Alford JS, Pieper RL, Huber FM (1989) Interaction of media components during bioreactor sterilizations: definition and importance of R_o. J Ind Microbiol 4:247–252
18. Boeck LD, Wetzel RW, Burt SC, Huber FM, Fowler GL, Alford JS (1988) Sterilization of bioreactor media on the basis of computer-calculated thermal input designated as F_o. J Ind Microbiol 3:305–310
19. Burley JR (1991) Don't overlook compact heat exchangers. Chem Eng 98(8):90–93, 95–96
20. Cacace D, Palmieri L, Pirone G, Dipollina G (1994) Biological validation of mathematical modeling of the thermal processing of particulate foods: the influence of heat transfer coefficient determination. J Food Eng 23:51–68
21. Cerf O, Davey KR, Sadoudi AK (1996) Thermal inactivation of bacteria- a new predictive model for the combined effect of three environmental factors: temperature, pH and water activity. Food Res Int 29(3–4):219–226
22. Chang SY, Toledo RT (1989) Heat transfer and simulated sterilization of particulate solids in a continuously flowing system. J Food Sci 54(4):1017–1023
23. Charm SL, Landau S, Williams B, Horowitz B, Prince AM, Pascual D (1992) High-temperature short-time heat inactivation of HIV and other viruses in human blood plasma. Vox Sang 62:12–20
24. Chisti Y, Moo-Young M (1994) Clean-in-place systems for industrial bioreactors: design, validation and operation. J Ind Microbiol 13:201–207
25. Churchill SW (1997) New wind in new bottles; unexpected findings in heat transfer Part IV Unexpected aspects of behavior for a double spiral heat exchanger. Thermal Sci Eng 5(4):11–27
26. Churchill SW (1977) Friction-factor equation spans all fluid-flow regimes. Chem Eng 84:91–92
27. Cinar A, Schlesser JE, Negiz A, Ramanauskas P, Armstrong DJ, Stroup W (eds) (1994) Automated control of thermal processes and dairy processing. In: Food Processing Automation III, American Society of Agricultural Engineers, St. Joseph, MI, pp158–167
28. Claeys L, Smout C, Van Loey AM, Henrickx ME (2004) From time temperature integrator kinetics to time temperature integrator tolerance levels: Heat-treated milk. Biotechnol Prog 20:1–12
29. Colebrook CF (1938–1939) Turbulent flow in pipes with particular reference to the transition region between the smooth and rough pipe laws. J Inst Civ Eng Lond 11:133–156
30. Cooney CL (1985) Media sterilization. In: Cooney CL, Humphrey AE (eds) Comprehensive biotechnology, Pergamon Press, NY, pp 296–297
31. Corbett K (1985) Design, preparation and sterilization of fermentation media. In: Moo-Young M (ed) Comprehensive biotechnology. Pergamon Press, NY, pp 127–139
32. Corredig M, Dangleish DG (1996) The binding of α-lactalbumin and β-lactoglobulin casein micelles in milk treated by different heating systems. Milchwissenschaft 51(3):123–127
33. Couvert O, Gaillard S, Savy N, Mafort P, Leguerinel I (2005) Survival curves of heated bacterial spores: effect of environmental factors on Weibull parameters. Int J Food Microbiol 101:73–81
34. Deindoerfer FH (1957) Calculation of heat sterilization times for fermentation media. Appl Microbiol 5:221–228
35. Deindoerfer FH, Humphrey AE (1959) Principles in the design of continuous sterilizers. Appl Microbiol 7:264–270
36. Foster D (1987) Scaling up in fermentation. Int Biotechnol Lab 5(2):18–23
37. Gallant RW, Railey JM (1984) Physical properties of hydrocarbons, vol 2, 2nd edn. Gulf Publishing Co., Houston, TX
38. Gilbert P, Brown G, Sandwith H (1979) A novel method for cleaning high temperature – short time pasteurizers. S Afr J Dairy Technol 11(2):57–59
39. Gilmour CH (1960) Application of heat exchangers in chemical plants. Ind Eng Chem 52(6):465–467
40. Grant IR, Hitchings EI, McCartney A, Ferguson F, Rowe MT (2002) Effect of commercial-scale high-temperature, short-time pasteurization on the viability of *Mycobacterium paratuberculosis* in naturally infected cows' milk. Appl Environ Microbiol 68(2):602–607
41. Gregoriades N, Luzardo M, Lucquet B, Ryll T (2003) Heat inactivation of mammalian cell cultures for biowaste kill system design. Biotechnol Prog 19:14–20
42. Gullart RW (1984) Physical properties of hydrocarbons, vol 2, 2nd edn. Gulf Publishing Co., Houston, TX, p 9
43. Hansen AP, Melo TS (1977) Effect of ultra-high temperature steam injection upon constituents of skim milk. J Dairy Sci 60:1368–1373
44. Harrod M (1990) Methods to distinguish between laminar and vortical flow in scraped surface heat exchangers. J Food Process Eng 13:39–57
45. Hasting A (1984) Practical engineering for biochemical applications. World Biotech Rep 3500:249–258
46. Heppell NJ (1985) Comparison of the residence time distributions of water and milk in an experimental UHT sterilizer. J Food Eng 4:71–84
47. Heppell NJ (1986) Comparison between the measured and predicted sterilization performance of a laboratory-scale, direct heated UHT plant. J Food Technol 21:385–399
48. Holman JP (1976) Heat Transfer, 4th edn. McGraw-Hill Co, NY
49. Hunter GM (1972) Continuous sterilization of liquid media containing suspended particles. Food Technol Aust 24(4):158–165
50. Janssen PWM (1994) Measurement of residence time distribution of processing plant using a cross correlation technique. J Food Eng 21:215–223
51. Junker B (2001) Technical evaluation of the potential for streamlining of equipment validation for fermentation applications. Biotechnol Bioeng 74(1):49–61
52. Junker BH, Beshty B, Wilson J (1999) Sterilization-in-place of concentrated nutrient solutions. Biotechnol Bioeng 62(5):501–508
53. Junker BH, Brix T, Lester M, Kardos P, Adamca J, Lynch J, Schmitt J, Salmon P (2003) Design and installation of a next generation pilot scale fermentation system. Biotechnol Prog 19:693–705

54. Kampen WH (1983) Industrial pilot plant. In: Vogel HC (eds) Fermentation and biochemical engineering handbook. Noyes Publications, Park Ridge, NJ
55. Kessler HG (1986) Considerations in relation to some technological and engineering aspects. IDF Bulletin 200, Chapter XV:80–86
56. Klees D (2002) Process description and feed forward control algorithm. Flow Control Mag 8(4):A4–A12
57. Kossik JM, Miller G (1994) Optimize cycle times for batch biokill systems. Chem Eng Prog 90(10):45–51
58. Kuman JD (1984) Cost update on specialty heat exchangers. Chem Eng 91(13):169–170, 172
59. Lee JH, Singh RW, Larkin JW (1990) Determination of lethality and processing time in a continuous sterilization system containing particulates. J Food Eng 11:67–92
60. Lee R, Waltz JW (1990) Consider continuous sterilization of bioprocess wastes. Chem Eng Prog 86(12):44–48
61. Levenspiel O (1958) Longitudinal mixing of fluids flowing in circular pipes. Ind Eng Chem 50(3):343–346
62. Levenspiel O (ed) (1962) Non-ideal flow. In: Chemical reaction engineering, Chap 9, 2nd edn. John Wiley and Sons, NY, pp253–325
63. Lin SH (1975) A theoretical analysis of thermal sterilization in a continuous sterilizer. J Ferment Technol 53(2):92–98
64. Liptak B (2000) Controller tuning: concepts and definitions. Control Magazine December:18
65. Lu Q, Piyasena P, Mittal GS (2001) Modeling alkaline phosphatase inactivation in bovine milk during high-temperature short-time pasteurization. Food Sci Technol Int 7(6):479–485
66. Lubiniecki AS, Gardner AR, Smith TM, Wang WK, McAllister PR, Federici MM (2003) Validation of fermentation processes. In: Brown F, Lubiniecki AS (eds) Process validation for manufacturing of biologics and biotechnology products, vol 113. Developments in Biologicals, Basel, Karger, pp37–44, 111–112
67. Mann A, Kiefer M, Leuenberger H (2001) Thermal sterilization of heat-sensitive products using high-temperature short-time sterilization. J Pharm Sci 90(3):275–287
68. McCabe W, Smith J (1976) Unit operations of chemical engineering, 3rd edn. McGraw-Hill, NY, p 52
69. McKellar RC, Modler HW, Couture H, Hughes A, Mayers P, Gleeson T, Ross WH (1994) Predictive modeling of alkaline phosphatase inactivation in a high-temperature short-time pasteurizer. J Food Prot 57(5):424–430
70. McMillan GK (ed) (2000) Cascade control tuning. In: Good tuning: a pocket guide, Chap 4. Instrument Society of America, NC, p 86
71. Minton PE (1970) Designing spiral-plate heat exchangers. Chem Eng 77:103–112
72. Nazarowec-White M, McKellar RC, Piyasena P (1999) Predictive modeling of *Enterobacter sakazakii* inactivation in bovine milk during high-temperature short-time pasteurization. Food Res Int 32:375–379
73. Ocio MJ, Fernandez PS, Rodrigo M, Periago P, Martinez A (1997) A time temperature integrator for particulated foods: thermal process evaluation. Z Lebensm-Unter und Forsh A 205:325–328
74. Oldfield DJ, Singh H, Taylor MW, Pearce KN (1998) Kinetics of denaturation and aggregation of whey proteins in skim milk heated in an ultra-high temperature (UHT) pilot plant. Int Dairy J 8:311–318
75. Olujic Z (1981) Compute friction factors fast for flow in pipes. Chem Eng 88(25):91–93
76. Palmicri L, Cacace D, Dipollina G, Dall'Aglio G, Masi P (1992) Residence time distribution of food suspensions containing large particles when flowing in tubular systems. J Food Eng 17:225–239
77. Patel R, Couch M, Pyle DL, Niranjan K, Varley J, Ashley MHJ, Fleming I, Hall A (1994) Direct steam injection sterilization of biological media: hydrodynamic and heat transfer studies. Trans I ChemE Part C 72(1):21–23
78. Perry RH, Chilton CH (1973) Chemical engineers' handbook, 5th edn. McGraw-Hill Book Company, NY, pp5–20, 5–21, 6–10
79. Pick AE (1982) Consider direct steam injection for heating liquids. Chem Eng 89(13):87–89
80. Piyasena P, Liou S, McKellar RC (1998) Predictive modelling of inactivation of *Listeria* spp in bovine milk during high-temperature short-time pasteurization. Int J Food Microbiol 39:167–173
81. Piyasena P, McKellar RC (1999) Influence of guar gum on the thermal stability of *Listeria innocua, Listeria monocytogenes*, and γ-glutamyl transpeptidase during high-temperature short-time pasteurization of bovine milk. J Food Prot 62(8):861–866
82. Piyasena P, McKellar RC, Bartlett FM (2003) Thermal inactivation of *Pediococcus* sp in simulated apple cider during high-temperature short-time pasteurization. Int J Food Microbiol 82:25–31
83. Rhodes A, Fletcher DL (1966) Principles of industrial microbiology. Pergamon Press, London
84. Roberts B, Rosen CG (1991) Safe disposal of biohazardous waste. Biotech Forum Eur 8(6):340–343
85. Rodrigo F, Rodrigo C, Fernandez PS, Rodrigo M, Martinez A (1999) Effect of acidification and oil on the thermal resistance of *Bacillus stearothermophilu*s spores heated in food substrate. Int J Food Microbiol 52:197–201
86. Rosemount Inc. (2004) Comprehensive product catalog, No. 00805-0100-1025, Rev. DA, Temperature section, p 157
87. Ross WH, Couture H, Hughes A, Mayers P, Gleeson T, McKellar RC (1998) A non-linear random coefficient model for the destruction of *Enterococcus faecium* in a high-temperature short-time pasteurizer. Food Microbiol 15:567–575
88. Rozema FR, Bos RRM, Boering G, van Asten JAAM, Nijenhuis AJ, Pennings AJ (1991) The effects of different steam-sterilization programs on material properties of poly (L-lactide). J Appl Biomater 2:23–28
89. Ruyter PW de, Brunet R (1973) Estimation of process conditions for continuous sterilization of foods containing particles. Food Technol 27(7):44–51
90. Sapru V, Smerage GH, Teixeira AA, Lindsay JA (1993) Comparison of predictive models for bacterial spore population resources to sterilization temperatures. J Food Sci 58(1):223–228
91. Schlesser JE, Armstrong DJ, Cinar A, Ramanauskas P, Negiz A (1997) Automated control and monitoring of thermal processing using high temperature, short time pasteurization. J Dairy Sci 80(10):2291–2296
92. Schlesser JE, Lynn G, Armstrong DJ, Cinar A, Ramanauskas P, Negiz A (1998) Acquisition, storage, and review of safety data from a commercial system for high temperature, short time pasteurization. J Dairy Sci 81(1):25–30
93. Sharma MC, Gurtu AK (1993) Asepsis in bioreactors. In: Niedleman S, Laskin AI (eds) Advances in applied microbiology. Academic Press Inc, NY, pp 1–27
94. Simon S, Mathiszik B, Mohr K-H (1992) Modelling and optimization of continuous sterilization processes. DECHEMA Biotechnol Conf 5:553–556
95. Singh RK (1988) Residence time distribution in aseptic processing. In: Nelson PE (ed) Principles of aseptic processing and packaging, Chap 3. Food Processors Institute, Washington, DC
96. Soderberg AC (1983) Fermentation design. In: Vogel HC (eds) Fermentation and biochemical engineering handbook. Noyes Publications, Park Ridge, NJ
97. Stanbury PF, Whitaker A (1984) Principles of fermentation technology. Pergamon Press, NY
98. Strantz AA, Zottola EA, Petran RL, Overdahl BJ, Smith LB (1989) The microbiology of sweet water and glycol cooling systems used in HTST pasteurizers in fluid milk processing plants in the United States. J Food Prot 52(11):799–804

99. Strenger MR, Churchill SW, Retallick WB (1990) Operational characteristics of a double-spiral heat exchanger for the catalytic incineration of contaminated air. Ind Eng Chem Res 29:1977–1984
100. Targett MJ, Betallick WB, Churchill SW (1992) Solutions in closed form for a double-spiral heat exchanger. Ind Eng Chem Res 31:658–669
101. Tejedor W, Rodrigo M, Martinez A (2001) Modeling the combined effect of pH and temperature on the heat resistance of *Bacillus stearothermophilus* spores heated in a multicomponent food extract. J Food Prot 64(10):1631–1635
102. Trinci APJ (1992) Myco-protein: a twenty-year overnight success story. Mycol Res 96(1):1–13
103. Trom L (1990) Consider plate and spiral heat exchangers. Hydrocarbon Proces 69(10):75–77
104. Trom L (1995) Use spiral plate exchangers for various applications. Hydrocarbon Proces 74(5):73–76, 78, 80
105. Wang DIC, Cooney CL, Demain AL, Dunnill P, Humphrey AE, Lilly M (1979) Fermentation and enzyme technology. John Wiley and Sons, NY, p 144
106. Zhivaikin LY, Blyakher IC, Shekhtman AA, Luk'yanenko ND, Alekseev VA, Budantsev PM (1982) Operational efficiency of spiral heat exchangers during heating and cooling of sulfuric acid. Soviet Chem Ind 14(6):757–760
107. Ziegler JG, Nichols NB (1942) Optimum settings for automatic controllers. ASME Trans 64:759